UNIVERSIDAD DE CONCEPCIÓN



Centro de Investigación en Ingeniería Matemática ($\mathrm{CI^2MA}$)



Resonant and non-resonant double Hopf bifurcation in a 4D Goodwin model with wage inequality

Daniel Cajas Guijarro, John Cajas Guijarro

PREPRINT 2025-25

SERIE DE PRE-PUBLICACIONES

Resonant and non-resonant double Hopf bifurcation in a 4D Goodwin model with wage inequality

John Cajas-Guijarro^a, Daniel Cajas-Guijarro^b

^aFacultad de Ciencias Económicas, Universidad Central del Ecuador; FLACSO-Ecuador, Quito, Ecuador

ARTICLE INFO

Keywords: Goodwin model Wage inequality Stability Double Hopf bifurcation Normal form Resonance

ABSTRACT

This paper presents a four-dimensional extension of the Goodwin model of endogenous cycles that integrates wage inequality and underemployment. The model distinguishes two classes of workers differentiated by productivity, wage levels, and bargaining strength, and endogenizes the underemployment rate through a simplified power-balance mechanism between capital and labor. We establish well-posedness of the system by proving existence-uniqueness of solutions, positivity, and forward invariance on a compact admissible set. The interior equilibrium is characterized in closed form and shown to generically undergo a double Hopf (Hopf-Hopf) bifurcation. Using center-manifold reduction and a third-order normal form, we derive the amplitude equations governing the interaction between two oscillatory modes (the Goodwin cycle and the underemployment cycle). The reduced dynamics predict the emergence of an invariant two-torus with quasi-periodic cycles and phase locking at low-order resonances (1:1, 1:2, 1:3). Numerical continuation and direct simulations corroborate the analytical predictions, documenting transitions between quasi-periodicity and resonant periodic orbits, and mapping the associated bifurcation structure in key parameters, such as the adjustment speed of the underemployment rate in response to deviations from steady-state equilibrium.

1. Introduction

Industrialized economies have experienced a marked rise in wage inequality since 1980, largely driven by the stagnation or decline of real wages among less-educated workers. In the United States, for example, the real earnings of male workers without a highschool diploma have fallen by approximately 15% between 1980 and 2017 [1, 2]. Empirical evidence also suggests that wage inequality is influenced by institutional and structural factors associated with labor markets, including union membership rates, unemployment benefits, and employment protection legislation [3, 4]. From a theoretical perspective, wage inequality has been examined within various economic frameworks. Neoclassical approaches commonly explain it as a consequence of skill-biased technical change, which enhances the productivity of high-skilled workers in the context of an unequal distribution of human capital across the population [5]. Other contributions within this tradition highlight the role of automation technologies that generate task displacement, meaning the substitution of lessskilled workers by machines capable of performing their tasks [2]. As noted in [6], these neoclassical perspectives tend to attribute wage inequality primarily to technological factors, considering labor market institutions only as amplifiers of their distributive consequences.

In contrast, heterodox approaches offer alternative explanations of the relationship among wage inequality, income distribution, and economic growth. Following [6] and [7], three broad strands can be identified, primarily inspired by classical-Marxian and post-Keynesian frameworks. The first comprises two-class models, such as [8], in which the economy is divided between production workers and capitalist-managers. The latter receive both wage and profit income and display a higher propensity to save than production workers. The second encompasses three-class models, exemplified by [9], where production workers earn low wages devoted entirely to consumption, managers earn higher wages that allow partial saving, and capitalists receive profit income and exhibit the highest propensity to save. The third strand is characterized by the division of the working class into two heterogeneous groups, either as a result of institutional factors such as labor market flexibility [10], or due to an unequal distribution of human capital, such as education, which differentiates workers into low- and high-skilled categories, with the latter exhibiting higher productivity and wage levels [11].

One of the most recent contributions within this third heterodox strand is presented in [6], which develops a model that describes the interaction between induced technical change driven by labor costs¹ and the dynamics of low- and high-skilled labor within a classical-Marxian framework enriched with Kaleckian elements. This model assumes a fixed-coefficient technology in which low-skilled

labor, high-skilled labor, and capital are complementary inputs in production. Low-skilled workers receive lower wages than highskilled workers, who are able to save a fraction of their income, while capitalists earn profits and save all of their income. Firms set prices by applying a mark-up over unit labor costs, with the mark-up decreasing as the employment rate of high-skilled workers rises. The nominal wage of low-skilled workers grows at a constant exogenous rate, reflecting the assumption of infinitely elastic labor supply, whereas the nominal wage growth of high-skilled workers depends positively on their employment rate. Combining these elements yields a threedimensional dynamical system in which the output-capital ratio, the wage differential, and the employment rate of high-skilled workers are state variables. The model exhibits a stable equilibrium point, and it shows that when the equilibrium wage differential exceeds a critical threshold, an exogenous increase in either the mark-up or the bargaining power of high-skilled workers enables both capitalists and high-skilled workers to expand their income shares at the expense of low-skilled workers.

Another strand of heterodox contributions to the study of wage inequality, although less explored, arises from works directly inspired by the Goodwin model of endogenous cycles and persistent unemployment [14].² For example, in [32] the original Goodwin framework is modified to incorporate the coexistence of a normalincome labor market (type 1 labor) and a low-income labor market (type 2 labor). The model uses a production function that allows for substitution between the two types of labor, with the marginal productivity of labor in each market determining the corresponding real wage, similar to the neoclassical model of exogenous growth [33]. The model also assumes that the growth rate of the real wage for type 1 labor depends positively on its employment rate and on the real wage of type 2 labor, capturing a reservation wage effect whereby type 1 workers who lose their jobs transition into type 2 positions. The real wage of type 2 workers, in turn, is defined as a fixed proportion of the real wage of type 1 labor, augmented by a component positively related to the employment rate of type 1 labor. From these elements, a two-dimensional dynamical system emerges in which the real wage of type 1 labor and the ratio of type 1 employment to capital serve as the state variables. The system is locally stable when the reservation wage effect is sufficiently weak but undergoes a Hopf bifurcation as

^bCI²MA and Departamento de Ingeniería Matemática, Concepción, Chile

 $[\]begin{tabular}{ll} \boxtimes jcajasg@uce.edu.ec (J. Cajas-Guijarro^a); dcajas2024@udec.cl (D. Cajas-Guijarro^b) \end{tabular}$

 $[\]text{ORCID}(s)$: 0000-0002-5753-0315 (J. Cajas-Guijarro"); 0009-0006-1968-7211 (D. Cajas-Guijarro")

¹For an analytical discussion of the induced innovation hypothesis, see [12, 13].

²The Goodwin model [14] formalizes the Marxian intuition that distributive conflict between workers and capitalists can generate endogenous cycles, manifested as persistent oscillations in the wage share–employment rate space. The model has inspired numerous extensions, including discussions about endogenous technical change [15, 16, 17], the active role of effective demand in long-run dynamics [18, 19, 20], inflation [21], two-sector interactions [22, 23], financial instability [24, 25], endogenous labor supply [26], inclusion of unemployment benefit systems and a minimum wage [27], open-economy dynamics under balance-of-payments constraints [28], chaotic behavior [29, 30], among other developments. A comprehensive survey of the theoretical and empirical literature on endogenous cycles derived from the Goodwin model can be found in [31].

this effect approaches a critical threshold, marking a transition from damped oscillations to persistent or even explosive cycles.

In a more recent, albeit preliminary, contribution [35], it is proposed a model with exogenous productivity growth, in which highskilled workers always exhibit higher productivity than low-skilled workers. In this setting, the growth rate of the real wage for highskilled workers depends positively on their employment rate, whereas the real wage of low-skilled workers is defined as a fixed proportion of high skilled wages. The model further assumes that all social classes save, with low-skilled workers displaying the lowest propensity to save and capitalists the highest. Combining these elements yields a two-dimensional dynamical system in which the employment rate and the wage share of high-skilled workers serve as the state variables. The model preserves the analytical structure of the original Goodwin framework, implying the existence of closed orbits. Moreover, when a minimum wage is introduced or the wage gap is exogenously reduced, the amplitude of fluctuations diminishes for both state variables.⁴

Building on this line of research, the present paper extends the Goodwin model by coupling the dynamics of wage inequality and underemployment, interpreted here as a regime of low productivity, low wages, and weak bargaining power. The proposed model distinguishes two groups of workers who differ in terms of productivity, wage levels, and bargaining strength, and endogenizes the underemployment rate through a simplified power-balance mechanism between capitalist firms and workers. This formulation yields a four-dimensional dynamical system in which the wage share, the employment rate, the relative wage of type 2 workers, and the underemployment rate are the state variables. A novelty of the model is the emergence of a double Hopf bifurcation that generates two interacting endogenous oscillatory modes: the classical Goodwin cycle and an underemployment cycle. The analysis of the cubic normal form reveals both resonant and non-resonant regimes, corresponding to synchronized periodic or quasi-periodic oscillations, respectively. Numerical simulations corroborate these theoretical results, displaying multi-frequency patterns, resonance windows, and transitions between regular and irregular regimes. The paper thus contributes to the literature on endogenous macroeconomic fluctuations by offering a framework that connects distributive cycles and wage inequality within a heterodox analytical approach.

The remainder of the paper is organized as follows. Section 2 presents the formulation of the four-dimensional dynamical system. Section 3 establishes the existence and uniqueness of its solutions. Section 4 characterizes the steady-state equilibrium and demonstrates the existence of a double Hopf bifurcation. Section 5 examines the cubic normal form on the center manifold to assess local stability properties. Section 6 reports the results of numerical simulations for both resonant and non-resonant double Hopf bifurcations. Section 7 concludes by summarizing the main findings and outlining directions for future research.

2. Model Formulation

Similar to [32], consider a closed economy without government, composed of capitalists, type 1 workers (i = 1), and type 2 workers (i = 2). The two groups of workers differ due to structural asymmetries in productivity, wages, and bargaining power. Firms produce a single good used for both consumption and investment, employing labor and fixed capital. During the production process, labor is allocated between type 1 and type 2 workers according to the following equations:

$$q(t) = a_1(t)l_1(t) + a_2(t)l_2(t), (1)$$

$$q(t) = a_1(t)l_1(t) + a_2(t)l_2(t),$$

$$a_1(t) = a_0e^{\alpha t}, \quad a_2(t) = \varepsilon_a a_0e^{\alpha t},$$
(2)

where $a_0 > 0$ and $0 < \varepsilon_a < 1$. Here, q represents real output, produced by type 1 and type 2 workers, who are treated as perfect substitutes for analytical simplicity.⁵ The terms l_i and a_i denote, respectively, the total hours worked and the labor productivity of workers of type i. The term a_0 is the initial productivity of type 1 workers, while α captures an exogenous and uniform rate of productivity growth across both worker groups. The ratio $\varepsilon_a = a_2/a_1$ measures the productivity of type 2 labor relative to type 1 labor—hereafter referred to as type 2 relative productivity—under the assumption that type 1 workers are always more productive (ε_a < 1). For simplicity, both α and ε_a are treated as constant and exogenously determined parameters.⁶

Given the aggregate labor supply n, the overall employment rate of the economy, v, is defined as:

$$v(t) = \frac{l_1(t) + l_2(t)}{n(t)},\tag{3}$$

where 1 - v is the unemployment rate. To describe the composition of employed workers between type 1 and type 2 labor, the underemployment rate, z, is introduced as:

$$z(t) = \frac{I_2(t)}{I_1(t) + I_2(t)}. (4)$$

By combining equations (1) through (4), real output can be expressed

$$q(t) = a_0 e^{\alpha t} v(t) n(t) \left[1 - z(t)(1 - \varepsilon_a) \right]. \tag{5}$$

Assuming that labor supply grows at a constant rate,8

$$\hat{n}(t) := \beta > 0$$
,

log-differentiating equation (5) and rearranging terms yields:

$$\hat{v}(t) = \hat{q}(t) - (\alpha + \beta) + \hat{z}(t) \frac{z(t)(1 - \varepsilon_a)}{1 - z(t)(1 - \varepsilon_a)}.$$
(6)

Equation (6) shows how the underemployment rate (z) influences the dynamics of the overall employment rate (v), depending on type 2 relative productivity (ε_a) . It follows that z has no effect on v when the two types of labor exhibit identical productivity ($\epsilon_a = 1$).

Regarding income distribution, consider the following formula-

$$u(t) = \frac{w_1(t)l_1(t) + w_2(t)l_2(t)}{q(t)},$$

$$w_2(t) = \varepsilon_w(t) w_1(t), \quad 0 < \varepsilon_w < 1.$$
(8)

$$w_2(t) = \varepsilon_w(t) w_1(t), \quad 0 < \varepsilon_w < 1.$$
 (8)

Here, u represents the aggregate wage share, w_i denotes the real wage received by workers of type i, and ε_w is the relative wage of type 2 workers compared with type 1 workers—hereafter referred to as the type 2 relative wage—, which is assumed to be endogenous. Combining equations (3), (4), (5), (7), and (8), u can be expressed

$$u(t) = \frac{w_1(t) \left[1 - z(t)(1 - \varepsilon_w(t))\right]}{a_0 e^{\alpha t} \left[1 - z(t)(1 - \varepsilon_a)\right]}.$$
 (9)

Since ε_w is endogenous and evolves over time, log-differentiating equation (9) yields:

$$\begin{split} \hat{u}(t) &= \hat{w}_1(t) - \alpha + \varepsilon_w(t) \left[\frac{z(t) \, \varepsilon_w(t)}{1 - z(t)(1 - \varepsilon_w(t))} \right] \\ &+ \hat{z}(t) \left[\frac{z(t)(\varepsilon_w(t) - \varepsilon_a)}{[1 - z(t)(1 - \varepsilon_a)][1 - z(t)(1 - \varepsilon_w(t))]} \right]. \end{split} \tag{10}$$

³In [34] the model is further extended to incorporate an unemployment benefit system and minimum wages in the type 2 labor market, and a maximum wage constraint in the type 1 labor market.

⁴It is also possible to identify contributions that address wage inequality from the perspective of endogenous cycles, though incorporating several Kaleckian elements. These include an endogenous rate of capacity utilization that adjusts to disequilibrium in the goods market, an investment function independent of savings, and mark-up pricing. Some examples focused on two-dimensional dynamics include [36] and [37]

⁵The assumption of productive substitution between heterogeneous workers is also adopted in other models of wage inequality, such as [11] and [32].

⁶The assumption of a constant value for ε_a is also employed in [11] and [35]. Likewise, the assumption of a constant productivity growth rate α , implying exogenous technical change, is adopted in [35].

The term underemployment rate is used since type 2 workers are assumed to occupy lower-productivity, lower-wage positions characterized by weaker bargaining power, indicating employment conditions below the standard or normal level

⁸For any function x, its time derivative is x'(t) = dx/dt and its growth rate is

 $[\]hat{x}(t) = x'(t)/x(t)$.

⁹A similar assumption is adopted in [6].

Equation (10) shows how the underemployment rate (z) influences the dynamics of the wage share (u), depending on both type 2 relative productivity (ε_a) and the type 2 relative wage (ε_w).

To characterize the dynamics of ε_w , we assume that the growth rate of real wages for each type of labor $(\hat{u_i})$ depends positively on its participation in total labor supply (l_i/n) . This relationship is represented by the following real wage Phillips curves: ¹⁰

$$\hat{w}_1(t) = -\gamma + \rho\left(\frac{l_1(t)}{n(t)}\right) = -\gamma + \rho(1 - z(t))v(t), \tag{11}$$

$$\hat{w}_2(t) = -\gamma + \rho \varepsilon_{\rho} \left(\frac{l_2(t)}{n(t)} \right) = -\gamma + \rho \varepsilon_{\rho} z(t) v(t), \tag{12}$$

with $\gamma, \rho > 0$ and $0 < \varepsilon_{\rho} < 1$. In these expressions, γ denotes an autonomous tendency for real wages to stabilize, ρ captures the responsiveness of wage growth of type 1 workers to the employment share of type 1 labor (l_1/n) , and $\rho\varepsilon_{\rho}$ reflects the influence of the employment share of type 2 labor (l_2/n) on the real wage growth of type 2 workers. As suggested in [17], a lower γ or a higher ρ signals an exogenous strengthening of the bargaining power of the working class. Meanwhile, the parameter ε_{ρ} is interpreted as an indicator of the specific bargaining power of type 2 workers, shaped by the structural disadvantages they face in wage negotiations. These disadvantages may arise from lower unionization rates, social or historical discrimination, or weaker collective bargaining institutions that erode the bargaining position of type 2 workers relative to type 1 workers ($\varepsilon_{\rho} < 1$).

By log-differentiating equation (8) and substituting equations (11) and (12), we derive a dynamic equation for ε_w :

$$\hat{\varepsilon}_{w}(t) = \rho \left[z(t)(1 + \varepsilon_{\rho}) - 1 \right] v(t). \tag{13}$$

Furthermore, substituting equation (11) into (10) provides an expression describing the dynamics of the aggregate wage share (\hat{u}) :

$$\begin{split} \hat{u}(t) &= -(\gamma + \alpha) + \rho(1 - z(t))v(t) \\ &+ \hat{\varepsilon}_w(t) \left[\frac{z(t)\varepsilon_w(t)}{1 - z(t)(1 - \varepsilon_w(t))} \right] \\ &+ \hat{z}(t) \left[\frac{z(t)(\varepsilon_w(t) - \varepsilon_a)}{[1 - z(t)(1 - \varepsilon_a)][1 - z(t)(1 - \varepsilon_w(t))]} \right]. \end{split}$$

$$(14)$$

Concerning capitalist accumulation, we follow the interpretation of the Goodwin model [14] as presented in [38]. Capitalists are assumed to save a fixed proportion s ($0 < s \le 1$) of their profits, q(1-u), which is entirely devoted to investment. In contrast, both type 1 and type 2 workers consume their entire wage income. If the capital-output ratio is defined as $\sigma = k/q$, where σ is an exogenous constant, and δ denotes the depreciation rate ($0 < \delta < 1$), the capital stock growth rate (\hat{k}) can be expressed as:

$$\hat{k}(t) = \frac{s(1 - u(t))}{\sigma} - \delta. \tag{15}$$

Since the capital-output ratio σ is constant, it follows that $\hat{k} = \hat{q}$. Substituting this result into equation (6) and combining with equation (15) yields the following expression for the dynamics of the employment rate (\hat{n}) :

$$\hat{v}(t) = \frac{s(1 - u(t))}{\sigma} - (\alpha + \beta + \delta) + \hat{z}(t) \left[\frac{z(t)(1 - \varepsilon_a)}{1 - z(t)(1 - \varepsilon_a)} \right]. \quad (16)$$

Finally, we assume that the underemployment rate (z) adjusts whenever the observed type 2 relative wage (ε_w) deviates from an equilibrium value (ε_w^0) . This behavior is represented by the following reduced-form dynamic equation:

$$\hat{z}(t) = \chi \left(\varepsilon_w^0 - \varepsilon_w(t)\right), \quad \chi > 0, \quad 0 < \varepsilon_w^0 < 1.$$
 (17)

where χ measures the adjustment speed of the underemployment rate. Equation (17) reflects the assumption that, on average, when the observed type 2 relative wage falls below its equilibrium value ($\varepsilon_w^0 > \varepsilon_w$), capitalist firms are motivated to increase the underemployment rate ($\hat{z} > 0$) to take advantage of the lower cost of type 2 labor. Conversely, when the observed type 2 relative wage exceeds its

¹⁰From equations (3) and (4), we note that $l_1/n = (1-z)v$ and $l_2/n = zv$.

equilibrium value ($\epsilon_w^0 < \epsilon_w$), type 2 workers obtain relatively higher wages, strengthening the bargaining position of the working class as a whole and exerting downward pressure on underemployment ($\hat{z} < 0$).

The mechanism represented in equation (17) captures the balance of power between capital and labor in determining the degree of underemployment. The parameters χ and ε_w^0 summarize structural and institutional conditions-such as labor market regulation, employment protection, and union strength—that shape both the ability of capitalists to substitute type 1 workers with type 2 workers and the capacity of the working class to defend its employment conditions. This formulation is consistent with Kalecki's view that capitalist economies are characterized by an inherent tension between profitability and full employment. As emphasized by Kalecki [39], prolonged periods of high employment and rising real wages undermine capitalist authority while strengthening the economic and political power of the working class. In this sense, equation (17) formalizes Kalecki's insight that maintaining a certain degree of labor market slack, embodied in the persistence of underemployed labor, constitutes a strategic element of capitalist stability.

Equations (13), (14), (16), and (17) form a four-dimensional dynamical system with the wage share (u), the employment rate (v), the underemployment rate (z), and the type 2 relative wage (ϵ_w) as state variables.

3. Existence and Uniqueness of Dynamic Trajectories

This section establishes the existence and uniqueness of the solutions to the model introduced in the previous section, using fixed-point theory. This result guarantees that, for any admissible initial conditions in terms of income distribution (u), employment (v), underemployment (z), and relative wages (ε_w) , the model yields a unique and continuous trajectory describing the evolution of the economy. Thus, for the subsequent results we shall work within the following domain. Let

$$\Gamma = \left\{ (X_1, X_2, X_3, X_4) \in \mathbb{R}_+^4 : \max_i |X_i| \le M \right\}, \qquad M > 0.$$

Fix any $\eta \in (0, 1)$ and define the admissible box

$$\Gamma_n = \{(u, v, z, \varepsilon_w) \in \Gamma : D_a, D_w \ge \eta\},$$

with
$$D_a := 1 - z(1 - \varepsilon_a)$$
 and $D_w := 1 - z(1 - \varepsilon_w)$.

Theorem 1. Define the state vector as: $\mathbf{X}(t) = (u(t), v(t), z(t), \varepsilon_w(t))^{\mathsf{T}}$. Assume moreover that $\sigma > 0$. Then, for every $\mathbf{X}^0 \in \Gamma_\eta$, the model of (13), (14), (16), and (17) under the initial value \mathbf{X}^0 exhibits a unique solution \mathbf{X}

PROOF. Since we work with growth rates, defined by $\hat{x}(t) = x'(t)/x(t)$, we can set $f = (f_1, f_2, f_3, f_4)$ where:

$$\begin{split} f_1(u,v,z,\varepsilon_w) &:= -(\gamma+\alpha) + \rho(1-z)\,v + \rho\left[z(1+\varepsilon_\rho)-1\right]v\frac{z\,\varepsilon_w}{D_w} \\ &\quad + \chi(\varepsilon_w^0-\varepsilon_w)\frac{z(\varepsilon_w-\varepsilon_a)}{D_aD_w}, \\ f_2(u,v,z,\varepsilon_w) &:= \frac{s(1-u)}{\sigma} - (\alpha+\beta+\delta) \\ &\quad + \chi(\varepsilon_w^0-\varepsilon_w)\frac{z(1-\varepsilon_a)}{D_a}, \\ f_3(u,v,z,\varepsilon_w) &:= \chi(\varepsilon_w^0-\varepsilon_w), \\ f_4(u,v,z,\varepsilon_w) &:= \rho\left[z(1+\varepsilon_a)-1\right]v. \end{split}$$

Then, the system of ODEs can be written as:

$$u' = uf_1,$$
 $v' = vf_2,$ $z' = zf_3,$ $\varepsilon'_w = \varepsilon_w f_4,$

and, consequently we have the ODE field $F = (uf_1, vf_2, zf_3, \varepsilon_w f_4)$. Then, for arbitrary $\mathbf{X}, \tilde{\mathbf{X}} \in \Gamma$, we obtain

$$\begin{split} \|F(\mathbf{X}) - F(\tilde{\mathbf{X}})\| &= \left| uf_1(\mathbf{X}) - \tilde{u}f_1(\tilde{\mathbf{X}}) \right| + \left| vf_2(\mathbf{X}) - \tilde{v}f_2(\tilde{\mathbf{X}}) \right| \\ &+ \left| zf_3(\mathbf{X}) - \tilde{z}f_3(\tilde{\mathbf{X}}) \right| + \left| \varepsilon_w f_4(\mathbf{X}) - \tilde{\varepsilon}_w f_4(\tilde{\mathbf{X}}) \right|. \end{split}$$

In general, for arbitrary scalars $a, b, \tilde{a}, \tilde{b}$, the following inequality holds:

$$\left|ab - \tilde{a}\tilde{b}\right| = \left|ab - \tilde{a}b + \tilde{a}b - \tilde{a}\tilde{b}\right| \le \left|a - \tilde{a}\right| \, \left|b\right| + \left|\tilde{a}\right| \left|b - \tilde{b}\right|, \quad (P1)$$

and in our setting, we obtain:

$$\begin{split} \|F(\mathbf{X}) - F(\tilde{\mathbf{X}})\| &\leq |u - \tilde{u}| \left| f_1(\mathbf{X}) \right| + |\tilde{u}| \left| f_1(\mathbf{X}) - f_1(\tilde{\mathbf{X}}) \right| \\ &+ |v - \tilde{v}| \left| f_2(\mathbf{X}) \right| + |\tilde{v}| \left| f_2(\mathbf{X}) - f_2(\tilde{\mathbf{X}}) \right| \\ &+ |z - \tilde{z}| \left| f_3(\mathbf{X}) \right| + |\tilde{z}| \left| f_3(\mathbf{X}) - f_3(\tilde{\mathbf{X}}) \right| \\ &+ |\varepsilon_w - \tilde{\varepsilon}_w| \left| f_4(\mathbf{X}) \right| + |\tilde{\varepsilon}_w| \left| f_4(\mathbf{X}) - f_4(\tilde{\mathbf{X}}) \right|. \end{split}$$

To estimate these terms, we consider on Γ_{η} we have $u,v,z,\varepsilon_w \leq M$ and $D_a,D_w \geq \eta$. These conditions allow us to derive the following bounds:

$$\begin{split} |f_{1}(\mathbf{X})| &\leq |\gamma| + |\alpha| + |\rho| \, |1-z| \, |v| + |\rho| \, (|z|(1+\varepsilon_{\rho})+1) \, |v| \, \frac{|z| \, \varepsilon_{w}}{D_{w}} \\ &+ |\chi| \, |\varepsilon_{w}^{0} - \varepsilon_{w}| \, \frac{|z| \, |\varepsilon_{w} - \varepsilon_{a}|}{D_{a} D_{w}} \\ &\leq |\gamma| + |\alpha| + |\rho| (1+M)M + |\rho| \, (|1+\varepsilon_{\rho}| \, M+1) M \, \frac{M^{2}}{\eta} \\ &+ |\chi| (|\varepsilon_{w}^{0}| + M) \, \frac{M(M+|\varepsilon_{a}|)}{\eta^{2}} \\ &= : b_{1}. \\ |f_{2}(\mathbf{X})| &\leq \frac{|s|}{|\sigma|} \, |1-u| + |\alpha+\beta+\delta| + |\chi| \, |\varepsilon_{w}^{0} - \varepsilon_{w}| \, \frac{|z| \, |1-\varepsilon_{a}|}{D_{a}} \\ &\leq \frac{|s|}{|\sigma|} (1+M) + |\alpha+\beta+\delta| + |\chi| \, (|\varepsilon_{w}^{0}| + M) \, \frac{M \, |1-\varepsilon_{a}|}{\eta} \\ &= : b_{2}. \end{split}$$

$$\begin{split} |f_3(\mathbf{X})| &\leq |\chi| \left(|\varepsilon_w^0| + |\varepsilon_w| \right) \leq |\chi| \left(|\varepsilon_w^0| + M \right) = \colon b_3. \\ |f_4(\mathbf{X})| &\leq |\rho| \left(|z| (1+\varepsilon_\rho) + 1 \right) |v| \leq |\rho| \left(|1+\varepsilon_\rho| \, M + 1 \right) M = \colon b_4. \end{split}$$

We now consider the difference, which yields:

$$\begin{split} \left| f_1(\mathbf{X}) - f_1(\tilde{\mathbf{X}}) \right| &\leq |\rho| \ |(1-z)v - (1-\tilde{z})\tilde{v}| \\ &+ |\rho| \ \left| \left(z(1+\varepsilon_\rho) - 1 \right) v H_1 - \tilde{H}_1 \tilde{v} \left(\tilde{z}(1+\varepsilon_\rho) - 1 \right) \right| \\ &+ |\chi| \ \left| (\varepsilon_w^0 - \varepsilon_w) H_2 - (\varepsilon_w^0 - \tilde{\varepsilon}_w) \tilde{H}_2 \right|, \end{split}$$

where $H_1:=\frac{z\,\varepsilon_w}{D_w}$ and $H_2:=\frac{z(\varepsilon_w-\varepsilon_a)}{D_aD_w}$. We now proceed to analyze the expression term by term:

• For the product, applying (1), we obtain:

$$\begin{split} |(1-z)v - (1-\tilde{z})\tilde{v}| &\leq |1-z| \ |v-\tilde{v}| + |\tilde{v}| \ |z-\tilde{z}| \\ &\leq (1+M) \, |v-\tilde{v}| + M \, |z-\tilde{z}| \, . \end{split}$$

• For the subsequent term, we use the fact that

$$f_4(\mathbf{X}) := \rho \left[z(1 + \epsilon_a) - 1 \right] v$$

so that, by applying (1), we obtain

$$\begin{aligned} \left| f_4(\mathbf{X}) H_1 - f_4(\tilde{\mathbf{X}}) \, \tilde{H}_1 \right| &\leq \left| f_4(\mathbf{X}) - f_4(\tilde{\mathbf{X}}) \right| \, \left| H_1 \right| \\ &+ \left| f_4(\tilde{\mathbf{X}}) \right| \, \left| H_1 - \tilde{H}_1 \right|. \end{aligned}$$

Here for $|H_1 - \tilde{H}_1|$, we again make use of (1), and additionally consider the fact that |b|, $|\tilde{b}| \ge \eta > 0$. In this case we obtain

$$\left| a\frac{1}{b} - \tilde{a}\frac{1}{\tilde{b}} \right| \le |a - \tilde{a}| \frac{1}{|b|} + |\tilde{a}| \left| \frac{b - \tilde{b}}{b\tilde{b}} \right|$$

$$\le \frac{|a - \tilde{a}|}{n} + \frac{|\tilde{a}|}{n^2} |b - \tilde{b}|.$$
(P2)

In our setting, this leads to

$$\left|z\,\varepsilon_w\frac{1}{D_w}-\tilde{z}\,\tilde{\varepsilon}_w\frac{1}{\tilde{D}}\right|\leq \frac{\left|z\,\varepsilon_w-\tilde{z}\,\tilde{\varepsilon}_w\right|}{\eta}+\frac{\left|\tilde{z}\,\tilde{\varepsilon}_w\right|}{\eta^2}\,\left|D_w-\tilde{D}_w\right|,$$

Since inequality (1) will be used repeatedly in what follows, we mention it only once here and apply it to each case without restating it, in particular:

$$\left|z\varepsilon_{w}-\tilde{z}\,\tilde{\varepsilon}_{w}\right|\leq\left|z-\tilde{z}\right|M+M\left|\varepsilon_{w}-\tilde{\varepsilon}_{w}\right|.$$

Moreover, since $|\tilde{z}\,\tilde{\varepsilon}_{m}^{2}| \leq M^{2}$ and combining this with

$$|D_w - \tilde{D}_w| = |z(1 - \varepsilon_w) - \tilde{z}(1 - \tilde{\varepsilon}_w)|$$

 $\leq (1+M)|z-\tilde{z}|+M|\varepsilon_w-\tilde{\varepsilon}_w|,$

we obtain, after substitution,

$$\begin{split} \left| H_1 - \tilde{H}_1 \right| &\leq \left(\frac{M}{\eta} + \frac{M^2(1+M)}{\eta^2} \right) |z - \tilde{z}| \\ &+ \left(\frac{M}{\eta} + \frac{M^3}{\eta^2} \right) \left| \varepsilon_w - \tilde{\varepsilon}_w \right| \\ &\leq K_{H_1} \left(|z - \tilde{z}| + \left| \varepsilon_w - \tilde{\varepsilon}_w \right| \right), \end{split}$$

where one may take

$$K_{H_1} := \max \left\{ \frac{M}{\eta} + \frac{M^2(1+M)}{\eta^2}, \frac{M}{\eta} + \frac{M^3}{\eta^2} \right\}.$$

Now, for the final expression

$$\begin{split} \left| f_4(\mathbf{X}) - f_4(\tilde{\mathbf{X}}) \right| &= |\rho| \, \left| [z(1+\varepsilon_\rho) - 1]v - [\tilde{z}(1+\varepsilon_\rho) - 1]\tilde{v} \right| \\ &\leq |\rho| \, \left(M|1+\varepsilon_\rho| + 1 \right) \, |v - \tilde{v}| \\ &+ |\rho| \, M \, |1+\varepsilon_\rho| \, |z - \tilde{z}| \\ &\leq \tau_v^{(4)} \, |v - \tilde{v}| + \tau_v^{(4)} \, |z - \tilde{z}| \, , \end{split}$$

where

$$\tau_{v}^{(4)} := |\rho| \left(M | 1 + \varepsilon_{o}| + 1 \right), \qquad \tau_{c}^{(4)} := |\rho| M | 1 + \varepsilon_{o}|.$$

Now we can finally replace in our original expression:

$$\begin{split} \left| f_4(\mathbf{X}) H_1 - f_4(\tilde{\mathbf{X}}) \; \tilde{H}_1 \right| &\leq \frac{M^2}{\eta} \, \tau_v^{(4)} \, |v - \tilde{v}| \\ &+ \left(\tau_z^{(4)} + b_4 \, K_{H_1} \right) |z - \tilde{z}| \\ &+ b_4 \, K_{H_1} \left| \varepsilon_w - \tilde{\varepsilon}_w \right|. \end{split}$$

• For the last term, we have:

$$\begin{split} \left| (\varepsilon_w^0 - \varepsilon_w) H_2 - (\varepsilon_w^0 - \tilde{\varepsilon}_w) \tilde{H}_2 \right| &\leq \left| \varepsilon_w - \tilde{\varepsilon}_w \right| \left| \tilde{H}_2 \right| \\ &+ \left(\left| \varepsilon_w^0 \right| + M \right) \left| H_2 - \tilde{H}_2 \right| \end{split}$$

we actually know the bound of $|\tilde{H}_2|$ from before,

$$\left| \tilde{H}_2 \right| \leq \frac{M \left(M + \left| \varepsilon_a \right| \right)}{\eta^2}$$

and using (2) with $a=z(\varepsilon_w-\varepsilon_a)$ and $b=D_aD_w$ where |b| , $|\tilde{b}|\geq\eta^2>0$ so:

$$\left|H_2 - \tilde{H}_2\right| \le \frac{|a - \tilde{a}|}{n^2} + \frac{|\tilde{a}|}{n^4} \left|b - \tilde{b}\right|.$$

where:

$$\begin{split} |a-\tilde{a}| &= \left|z(\varepsilon_w - \varepsilon_a) - \tilde{z}(\tilde{\varepsilon}_w - \varepsilon_a)\right| \\ &\leq \left(M + \left|\varepsilon_a\right|\right) |z - \tilde{z}| + M \left|\varepsilon_w - \tilde{\varepsilon}_w\right|, \end{split}$$

and $|\tilde{a}| \leq M(M + |\varepsilon_a|)$. For $|b - \tilde{b}|$ we directly have:

$$\begin{aligned} \left| b - \tilde{b} \right| &= \left| D_a D_w - \tilde{D}_a \tilde{D}_w \right| \\ &\leq \left| D_a \right| \left| D_w - \tilde{D}_w \right| + \left| \tilde{D}_w \right| \left| D_a - \tilde{D}_a \right|, \end{aligned}$$

where the bound for $\left|D_w-\tilde{D}_w\right|$ is already known from above and from a direct calculation we get:

$$\begin{split} \left|D_a - \tilde{D}_a\right| &= \left|(1 - \varepsilon_a)(\tilde{z} - z)\right| = \left|1 - \varepsilon_a\right| \, \left|z - \tilde{z}\right|, \\ \left|D_a\right| &\leq 1 + M \left|1 - \varepsilon_a\right|, \\ \left|D_m\right| &\leq 1 + M (1 + M). \end{split}$$

Then,

$$\begin{split} \left|b-\tilde{b}\right| &\leq \left(1+M|1-\varepsilon_{a}|\right) \, \left((1+M)\left|z-\tilde{z}\right|+M\left|\varepsilon_{w}-\tilde{\varepsilon}_{w}\right|\right) \\ &+ \left(1+M(1+M)\right) \, \left(\left|1-\varepsilon_{a}\right|\,\left|z-\tilde{z}\right|\right) \\ &\leq C_{b}^{(z)}\,\left|z-\tilde{z}\right|+C_{b}^{(w)}\,\left|\varepsilon_{w}-\tilde{\varepsilon}_{w}\right|, \end{split}$$

with the explicit constants.

$$\begin{split} C_b^{(z)} &:= (1+M|1-\varepsilon_a|)(1+M) + (1+M(1+M))|1-\varepsilon_a|, \\ C_b^{(w)} &:= (1+M|1-\varepsilon_a|)M. \end{split}$$

Therefore

$$\begin{split} \left| H_2 - \tilde{H}_2 \right| &\leq \left[\frac{M + |\varepsilon_a|}{\eta^2} + \frac{M(M + |\varepsilon_a|)}{\eta^4} \, C_b^{(z)} \right] |z - \tilde{z}| \\ &+ \left[\frac{M}{\eta^2} + \frac{M(M + |\varepsilon_a|)}{\eta^4} \, C_b^{(w)} \right] |\varepsilon_w - \tilde{\varepsilon}_w| \\ &\leq K_{H_2} \left(|z - \tilde{z}| + |\varepsilon_w - \tilde{\varepsilon}_w| \right), \end{split}$$

where we may set $K_{H_2} := \max\{K_{H_2}^{(z)}, K_{H_2}^{(w)}\}$, with

$$\begin{split} K_{H_2}^{(z)} &:= \frac{M + |\varepsilon_a|}{\eta^2} + \frac{M(M + |\varepsilon_a|)}{\eta^4} \, C_b^{(z)}, \\ K_{H_2}^{(w)} &:= \frac{M}{\eta^2} + \frac{M(M + |\varepsilon_a|)}{\eta^4} \, C_b^{(w)}. \end{split}$$

Now we can finally replace on:

$$\begin{split} \left| (\varepsilon_w^0 - \varepsilon_w) H_2 - (\varepsilon_w^0 - \tilde{\varepsilon}_w) \tilde{H}_2 \right| &\leq \left| \varepsilon_w - \tilde{\varepsilon}_w \right| \frac{M \left(M + \left| \varepsilon_a \right| \right)}{\eta^2} \\ &+ \left| z - \tilde{z} \right| \left(\left| \varepsilon_w^0 \right| + M \right) K_{H_2} \\ &+ \left| \varepsilon_w - \tilde{\varepsilon}_w \right| \left(\left| \varepsilon_w^0 \right| + M \right) K_{H_2}. \end{split}$$

We now return to the bound for $|f_1(\mathbf{X}) - f_1(\tilde{\mathbf{X}})|$, and by combining the preceding estimates we obtain:

$$\begin{split} \left| f_1(\mathbf{X}) - f_1(\tilde{\mathbf{X}}) \right| &\leq \left| \rho \right| \left((1+M) \left| v - \tilde{v} \right| + M \left| z - \tilde{z} \right| \right) \\ &+ \frac{M^2}{\eta} \tau_v^{(4)} \left| v - \tilde{v} \right| + \left(\tau_z^{(4)} + b_4 \, K_{H_1} \right) \left| z - \tilde{z} \right| \\ &+ b_4 \, K_{H_1} \left| \varepsilon_w - \tilde{\varepsilon}_w \right| + \left| \chi \right| \left| \varepsilon_w - \tilde{\varepsilon}_w \right| \frac{M \left(M + \left| \varepsilon_a \right| \right)}{\eta^2} \\ &+ \left| \chi \right| \left| z - \tilde{z} \right| \left(\left| \varepsilon_w^0 \right| + M \right) K_{H_2} \\ &+ \left| \chi \right| \left| \varepsilon_w - \tilde{\varepsilon}_w \right| \left(\left| \varepsilon_w^0 \right| + M \right) K_{H_2}, \end{split}$$

and after grouping terms appropriately:

$$\left| f_1(\mathbf{X}) - f_1(\tilde{\mathbf{X}}) \right| \le \tau_v^{(1)} \left| v - \tilde{v} \right| + \tau_z^{(1)} \left| z - \tilde{z} \right| + \tau_\varepsilon^{(1)} \left| \varepsilon_w - \tilde{\varepsilon}_w \right|,$$

where:

$$\begin{split} & \boldsymbol{\tau}_{\boldsymbol{v}}^{(1)} \, \vcentcolon= |\rho|(1+M) + \frac{M^2}{\eta} \, \boldsymbol{\tau}_{\boldsymbol{v}}^{(4)}, \\ & \boldsymbol{\tau}_{\boldsymbol{z}}^{(1)} \, \vcentcolon= |\rho|M + \boldsymbol{\tau}_{\boldsymbol{z}}^{(4)} + b_4 \, K_{H_1} + |\chi| \, \left(|\boldsymbol{\varepsilon}_{\boldsymbol{w}}^0| + M\right) K_{H_2}, \\ & \boldsymbol{\tau}_{\boldsymbol{\varepsilon}_{\boldsymbol{w}}}^{(1)} \, \vcentcolon= b_4 \, K_{H_1} + |\chi| \, \left(\frac{M \, (M + |\boldsymbol{\varepsilon}_{\boldsymbol{a}}|)}{\eta^2} + \left(|\boldsymbol{\varepsilon}_{\boldsymbol{w}}^0| + M\right) K_{H_2}\right). \end{split}$$

Now for the bound of $|f_2(\mathbf{X}) - f_2(\tilde{\mathbf{X}})|$ we proceed like this:

$$\left| f_2(\mathbf{X}) - f_2(\tilde{\mathbf{X}}) \right| \leq \left| \frac{s}{\sigma} \right| \left| |u - \tilde{u}| + |\chi| \left| (\varepsilon_w^0 - \varepsilon_w) H_3 - (\varepsilon_w^0 - \tilde{\varepsilon}_w) \tilde{H}_3 \right|,$$

where $H_3 = \frac{z(1 - \epsilon_a)}{D_a}$. From, (1) we can obtain,

$$\begin{split} \left| (\varepsilon_w^0 - \varepsilon_w) H_3 - (\varepsilon_w^0 - \tilde{\varepsilon}_w) \tilde{H}_3 \right| &\leq \left| \varepsilon_w - \tilde{\varepsilon}_w \right| \left| \tilde{H}_3 \right| \\ &+ \left(\left| \varepsilon_w^0 \right| + M \right) \left| H_3 - \tilde{H}_3 \right|. \end{split}$$

We already have an estimate for $|\tilde{H}_3|$

$$\left|\tilde{H}_{3}\right| \leq \frac{M\left|1-\varepsilon_{a}\right|}{\eta}.$$

Applying (2) with $a = z(1 - \varepsilon_a)$ and $b = D_a$, we obtain

$$\left|H_3-\tilde{H}_3\right| \leq \frac{\left|z-\tilde{z}\right|\left|1-\varepsilon_a\right|}{\eta} + \frac{M\left|1-\varepsilon_a\right|}{\eta^2} \, \left|D_a-\tilde{D}_a\right|.$$

From the previous bounds on $|D_a - \tilde{D}_a|$ it follows that

$$\left|H_3 - \tilde{H}_3\right| \leq |1 - \varepsilon_a| \left(\frac{1}{\eta} + \frac{M \left|1 - \varepsilon_a\right|}{\eta^2}\right) |z - \tilde{z}|.$$

Thus, we may take

$$K_{H_3} := |1 - \varepsilon_a| \left(\frac{1}{\eta} + \frac{M \, |1 - \varepsilon_a|}{\eta^2} \right).$$

Substituting this bound, we obtain

$$\begin{aligned} \left| (\varepsilon_w^0 - \varepsilon_w) H_3 - (\varepsilon_w^0 - \tilde{\varepsilon}_w) \tilde{H}_3 \right| &\leq \left| \varepsilon_w - \tilde{\varepsilon}_w \right| \frac{M \left| 1 - \varepsilon_a \right|}{\eta} \\ &+ \left| z - \tilde{z} \right| \left(\left| \varepsilon_w^0 \right| + M \right) K_{H_3} \end{aligned}$$

Finally, returning to $|f_2(\mathbf{X}) - f_2(\tilde{\mathbf{X}})|$, we obtain:

$$\begin{split} \left| f_2(\mathbf{X}) - f_2(\tilde{\mathbf{X}}) \right| &\leq \left| \frac{s}{\sigma} \right| \, |u - \tilde{u}| \\ &+ |\chi| \, \left| \varepsilon_w - \tilde{\varepsilon}_w \right| \, \frac{M \, |1 - \varepsilon_a|}{\eta} \\ &+ |\chi| \, |z - \tilde{z}| \, (|\varepsilon_w^0| + M) \, K_{H_2} \end{split}$$

and after grouping terms appropriately:

$$\left| f_2(\mathbf{X}) - f_2(\tilde{\mathbf{X}}) \right| \leq \tau_u^{(2)} \left| u - \tilde{u} \right| + \tau_z^{(2)} \left| z - \tilde{z} \right| + \tau_{\varepsilon_{\cdots}}^{(2)} \left| \varepsilon_w - \tilde{\varepsilon}_w \right|,$$

where:

$$\begin{split} \tau_u^{(2)} &:= \left|\frac{s}{\sigma}\right|, \qquad \tau_z^{(2)} := |\chi| \, \left(|\varepsilon_w^0| + M\right) K_{H_3}, \\ \tau_{\varepsilon_w}^{(2)} &:= |\chi| \, \, \frac{M \, |1 - \varepsilon_a|}{n}. \end{split}$$

Finally, for the remaining difference we directly obtain:

$$|f_3(\mathbf{X}) - f_3(\tilde{\mathbf{X}})| = |\chi| |\varepsilon_w - \tilde{\varepsilon}_w| \implies \tau_{\varepsilon_w}^{(3)} := |\chi|,$$

Gathering all the previous bounds, we now return to the main expression and obtain

$$\begin{split} \|F(\mathbf{X}) - F(\tilde{\mathbf{X}})\| &\leq |u - \tilde{u}| \left(b_1 + M \ \tau_u^{(2)}\right) \\ &+ |v - \tilde{v}| \left(b_2 + M \ \tau_v^{(1)} + M \ \tau_v^{(4)}\right) \\ &+ |z - \tilde{z}| \left(b_3 + M \ \tau_z^{(1)} + M \ \tau_z^{(2)} + M \ \tau_z^{(4)}\right) \\ &+ \left|\varepsilon_w - \tilde{\varepsilon}_w\right| \left(b_4 + M \ \tau_{\varepsilon_w}^{(1)} + M \ \tau_{\varepsilon_w}^{(2)} + M \ \tau_{\varepsilon_w}^{(3)}\right). \end{split}$$

If we now define $L := \max\{\theta_1, \theta_2, \theta_3, \theta_4\}$, where

$$\begin{split} \theta_1 &:= b_1 + M \, \tau_u^{(2)}, \\ \theta_2 &:= b_2 + M \, \tau_v^{(1)} + M \, \tau_v^{(4)}, \\ \theta_3 &:= b_3 + M \, \tau_z^{(1)} + M \, \tau_z^{(2)} + M \, \tau_z^{(4)}, \\ \theta_4 &:= b_4 + M \, \tau_z^{(1)} + M \, \tau_z^{(2)} + M \, \tau_z^{(3)}. \end{split}$$

we may write

$$||F(\mathbf{X}) - F(\tilde{\mathbf{X}})|| \le L ||\mathbf{X} - \tilde{\mathbf{X}}||.$$

Hence, F(X) satisfies the Lipschitz condition on X. By invoking the fixed point theorem, we conclude that Theorem (1) is established. \square

To complement this result on existence and uniqueness, we examine the following two propositions, which ensure that the system remains positive if it starts positive and that Γ_{η} is a forward-invariant set for the model

Proposition 1. Let $\mathbf{X}(t) = (u(t), v(t), z(t), \varepsilon_w(t))^{\mathsf{T}}$ be a solution to the system defined by equations (13), (14), (16), and (17). Write $F = (uf_1, vf_2, zf_3, \varepsilon_w f_4)$ as stated in Theorem (1). Then Γ_η is forward invariant if and only if $F(\bar{\mathbf{X}}) \in T(\Gamma_\eta; \bar{\mathbf{X}})$ for every $\bar{\mathbf{X}} \in \partial \Gamma_\eta$, where the contingent cone $T(\Gamma_\eta, \bar{\mathbf{X}})$ is

$$T\left(\Gamma_{\eta},\bar{\mathbf{X}}\right) \,:=\, \left\{ \begin{array}{l} h \in \mathbb{R}^4 \, \bigg| \, \exists \mathbf{X}_n \in \Gamma_{\eta} \,,\, \lambda_n > 0, \\ \mathbf{X}_n \to \bar{\mathbf{X}} \,,\, \lambda_n \, \left(\mathbf{X}_n - \bar{\mathbf{X}}\right) \to h \end{array} \right\}.$$

PROOF. We proceed to prove the double implication.

⇒) Assume Γ_{η} is forward invariant. Fix any $\bar{\mathbf{X}} \in \partial \Gamma_{\eta}$. Because the field is C^1 on a neighborhood of Γ_{η} by Theorem (1), there is a unique solution $\mathbf{X}(t)$ with $\mathbf{X}^0 := \bar{\mathbf{X}}$ and $\mathbf{X}(t) \in \Gamma_{\eta}$ for all $t \geq 0$. For a sequence $(t_n)_{n \geq 1} \subset (0, \infty)$ such that $t_{n+1} < t_n$ and $t_n \to 0$, set

$$\mathbf{X}_n := \mathbf{X}(t_n) \in \Gamma_{\eta}, \qquad \lambda_n := \frac{1}{t_n} > 0.$$

Then

$$\lambda_n \left(\mathbf{X}_n - \bar{\mathbf{X}} \right) = \frac{\mathbf{X}(t_n) - \mathbf{X}^0}{t_n}.$$

Now pass to the limit. Using the integral form of the ODE,

$$\mathbf{X}(t) - \mathbf{X}^0 = \int_0^t F(\mathbf{X}(s)) \ ds, \quad t \ge 0.$$

Hence, for each n.

$$\lambda_n \left(\mathbf{X}_n - \bar{\mathbf{X}} \right) = \frac{\mathbf{X}(t_n) - \mathbf{X}^0}{t_n} = \frac{1}{t_n} \int_0^{t_n} F\left(\mathbf{X}(s) \right) \, ds.$$

Therefore.

$$\left\| \lambda_n \left(\mathbf{X}_n - \bar{\mathbf{X}} \right) - F \left(\bar{\mathbf{X}} \right) \right\| = \left\| \frac{1}{t_n} \int_0^{t_n} F(\mathbf{X}(s)) \, ds - F(\bar{\mathbf{X}}) \right\|.$$

Because $\mathbf{X}(s) \to \mathbf{X}^0$ as $s \to 0$ and F is continuous at \mathbf{X}^0 , we have $F(\mathbf{X}(s)) \to F(\mathbf{X}^0)$. Therefore, for any $\varepsilon > 0$, there exists $\delta > 0$ such that

$$\left\| \mathbf{X}(s) - \mathbf{X}^0 \right\| < \delta \ \Rightarrow \ \left\| F\left(\mathbf{X}(s) \right) - F\left(\mathbf{X}^0 \right) \right\| < \varepsilon.$$

By continuity of **X** at 0, choose N with $t_n < \delta$ for all $n \ge N$. Then for $n \ge N$,

$$\left\| \lambda_n \left(\mathbf{X}_n - \bar{\mathbf{X}} \right) - F \left(\bar{\mathbf{X}} \right) \right\| \le \left\| \frac{1}{t_n} \int_0^{t_n} F \left(\mathbf{X}(s) \right) \, ds - F(\bar{\mathbf{X}}) \right\|$$

$$\le \frac{1}{t_n} \int_0^{t_n} \left\| F \left(\mathbf{X}(s) \right) - F \left(\mathbf{X}^0 \right) \right\| \, ds$$

$$< \varepsilon.$$

Since ε is arbitrary, we conclude that $\lambda_n \left(\mathbf{X}_n - \bar{\mathbf{X}} \right) \to F \left(\bar{\mathbf{X}} \right)$, hence $F \left(\bar{\mathbf{X}} \right) \in T \left(\Gamma_n; \bar{\mathbf{X}} \right)$.

 \Leftarrow) Assume that $F(\bar{\mathbf{X}}) \in T(\Gamma_{\eta}; \bar{\mathbf{X}})$ for every $\bar{\mathbf{X}} \in \partial \Gamma_{\eta}$. We prove that any solution starting in Γ_{η} never leaves. Let $\mathbf{X}(t)$ be the solution with $\mathbf{X}^0 \in \Gamma_{\eta}$ and define the function

$$\phi(t) := \operatorname{dist}(\mathbf{X}(t), \Gamma_{\eta}) = \inf_{y \in \Gamma_{\eta}} \|\mathbf{X}(t) - y\|.$$

Since Γ_{η} is closed, ϕ equals 0 exactly at those times for which $\mathbf{X}(t) \in \Gamma_{\eta}$. To reach a contradiction, suppose that \mathbf{X} leaves Γ_{η} .

$$T := \inf \left\{ t > 0 : \mathbf{X}(t) \notin \Gamma_n \right\} \in (0, \infty],$$

so that $\mathbf{X}(t) \in \Gamma_{\eta}$ for all t < T, and let $\mathbf{X}^* := \mathbf{X}(T) \in \partial \Gamma_{\eta}$. Because $F(\mathbf{X}^*) \in T(\Gamma_{\eta}; \mathbf{X}^*)$, by the definition of the contingent cone there exist

$$\mathbf{X}_n \in \Gamma_n$$
, $\lambda_n > 0$, $\mathbf{X}_n \to \mathbf{X}^*$, $\lambda_n (\mathbf{X}_n - \mathbf{X}^*) \to F(\mathbf{X}^*)$.

Fix $\varepsilon > 0$. By the above convergence, there exists N such that for all $n \ge N$,

$$\left\|\lambda_n(\mathbf{X}_n-\mathbf{X}^*)-F(\mathbf{X}^*)\right\|<\varepsilon.$$

Then we can choose $h_n := \lambda_n^{-1}$ sufficiently small so that

$$\|\mathbf{X}^* + h_n F(\mathbf{X}^*) - \mathbf{X}_n\| < \varepsilon h_n.$$

By the standard first-order expansion of the flow,

$$\mathbf{X}(T+h_n) = \mathbf{X}^* + h_n F(\mathbf{X}^*) + O(h_n), \quad \text{as } h_n \to 0.$$

Combining these two expressions in ϕ gives

$$\begin{split} \phi(T+h_n) &= \inf_{y \in \Gamma_n} \left\| \mathbf{X}(T+h_n) - y \right\| \\ &\leq \left\| \mathbf{X}(T+h_n) - \mathbf{X}_n \right\| \\ &< \varepsilon \; h_n + O(h_n). \end{split}$$

Then, the upper right Dini derivative satisfies

$$\phi'_{+}(T) := \limsup_{h \to 0^{+}} \frac{\phi(T+h) - \phi(T)}{h} < \varepsilon.$$

Since $\varepsilon > 0$ is arbitrary and $\phi(T) = 0$, we obtain $\phi'_+(T) \le 0$. However, if **X** were to exit at T, we would have $\phi(T+h) > 0$ for all sufficiently small h > 0, which would imply $\phi'_+(T) > 0$ a contradiction. Therefore, $\mathbf{X}(t) \in \Gamma_\eta$ for all $t \ge 0$, i.e., Γ_η is forward invariant.

Proposition 2. Let $\mathbf{X}(t) = (u(t), v(t), z(t), \varepsilon_w(t))^{\mathsf{T}}$ be a solution to the system defined by equations (13), (14), (16), and (17). If the initial condition $\mathbf{X}^0 \in \Gamma_w$, then the solution $\mathbf{X}(t)$ remains in Γ_n for all t > 0.

PROOF. On Γ_{η} , the vector field is of class C^1 and locally Lipschitz by Theorem (1). Therefore, for any initial condition $\mathbf{X}(0) \in \Gamma_{\eta}$, there exists a unique solution defined on a maximal interval [0,T) satisfying

$$\begin{split} u(t) &= u_0 e^{\int_0^t f_1(\mathbf{X}) \, ds}, & v(t) &= v_0 e^{\int_0^t f_2(\mathbf{X}) \, ds}, \\ z(t) &= z_0 e^{\int_0^t f_3(\mathbf{X}) \, ds}, & \varepsilon_w(t) &= \varepsilon_{w0} e^{\int_0^t f_4(\mathbf{X}) \, ds}. \end{split}$$

Consequently, $u,v,z,\varepsilon_w>0$ on [0,T). Moreover, by the bounds $|f_i|\leq b_i$ on Γ_η , no blow-up occurs before reaching $\partial\Gamma_\eta$. Hence, if $T<\infty$, then $\mathbf{X}(T)\in\partial\Gamma_\eta$. By Proposition (1), the set Γ_η is forward-invariant under the flow of the system. This invariance guarantees that a solution starting in Γ_η cannot reach the boundary $\partial\Gamma_\eta$ in finite time. Therefore, the solution $\mathbf{X}(t)$ remains in Γ_η for all t>0.

4. Steady State Equilibrium and Double Hopf Bifurcation

At the steady state $(\hat{u} = \hat{v} = \hat{z} = \hat{\varepsilon}_w = 0)$, the four-dimensional dynamical system defined by equations (13), (14), (16), and (17) admits the following non-trivial equilibrium point:

$$\dot{u} = 1 - \frac{\sigma(\alpha + \beta + \delta)}{s}, \qquad \dot{v} = \frac{(\alpha + \gamma)(1 + \varepsilon_{\rho})}{\rho \varepsilon_{\rho}},$$

$$\dot{z} = \frac{1}{1 + \varepsilon_{\rho}}, \qquad \varepsilon_{w} = \varepsilon_{w}^{0}.$$
(18)

The steady-state wage share, \dot{u} , coincides with the equilibrium value obtained in the Goodwin model with savings and depreciation, as formulated in [38]. It increases with the saving rate (s) and decreases with the capital-output ratio (σ), the rate of productivity growth (α), labor supply growth (β), and the depreciation rate (δ). The equilibrium employment rate, \dot{v} , rises with faster productivity growth (α) and stronger real wage stabilization (γ), but declines as the sensitivity of wage growth to type 1 employment (ρ) increases. Both \dot{v} and the equilibrium underemployment rate \dot{z} depend on the bargaining power of type 2 workers (ε_{ρ}): a lower ε_{ρ} raises \dot{v} while reducing \dot{z} , implying higher overall employment but deteriorated average labor conditions. Finally, the type 2 relative wage is fixed at its equilibrium value ($\dot{\varepsilon}_w = \varepsilon_w^0$).

Solving equations (13), (14), (16), and (17) for the time derivatives u', v', z', and ε'_w yields an autonomous dynamical system, which can be expressed in the following reduced form (as stated in Theorem (1))

$$u' = uf_1, \qquad v' = vf_2, \qquad z' = zf_3, \qquad \varepsilon'_w = \varepsilon_w f_4, \quad (19)$$

where f_i represents the function governing the dynamics of the state variable. Linearizing this dynamical system around the equilibrium point $\dot{\mathbf{X}} = (\dot{u}, \dot{v}, \dot{z}, \varepsilon_w)$, as defined in expression (18), gives:

$$\begin{pmatrix} u' \\ v' \\ z' \\ \varepsilon'_w \end{pmatrix} = \begin{pmatrix} 0 & A_{12} & A_{13} & A_{14} \\ A_{21} & 0 & 0 & A_{24} \\ 0 & 0 & 0 & A_{34} \\ 0 & 0 & A_{43} & 0 \end{pmatrix} \begin{pmatrix} u - \dot{u} \\ v - \dot{v} \\ z - \dot{z} \\ \varepsilon_w - \varepsilon_w \end{pmatrix},$$
 (20)

where.

$$\begin{split} A_{12} &= \frac{\varepsilon_{\rho} \rho [s - \sigma(\alpha + \beta + \delta)]}{s(1 + \varepsilon_{\rho})}, \\ A_{13} &= -\frac{(\alpha + \gamma)(1 - \varepsilon_{w}^{0})(1 + \varepsilon_{\rho})[s - \sigma(\alpha + \beta + \delta)]}{s(\varepsilon_{w}^{0} + \varepsilon_{\rho})}, \\ A_{14} &= \frac{\chi(\varepsilon_{a} - \varepsilon_{w}^{0})(1 + \varepsilon_{\rho})[s - \sigma(\alpha + \beta + \delta)]}{s(\varepsilon_{a} + \varepsilon_{\rho})(\varepsilon_{w}^{0} + \varepsilon_{\rho})}, \\ A_{21} &= -\frac{s(\alpha + \gamma)(1 + \varepsilon_{\rho})}{\varepsilon_{\rho} \rho \sigma}, \\ A_{24} &= -\frac{\chi(\alpha + \gamma)(1 - \varepsilon_{a})(1 + \varepsilon_{\rho})}{\varepsilon_{\rho}(\varepsilon_{a} + \varepsilon_{\rho})\rho}, \\ A_{34} &= -\frac{\chi}{1 + \varepsilon_{\rho}}, \end{split}$$

$$A_{43} = \frac{\varepsilon_w^0(\alpha + \gamma)(1 + \varepsilon_\rho)}{\varepsilon_\rho}^2.$$

The Jacobian matrix in equation (20) possesses four purely imaginary eigenvalues, expressed as $\lambda_{1,2} = \pm i\omega_1$ and $\lambda_{3,4} = \pm i\omega_2$, where:

$$\omega_1^2 = \frac{[s - \sigma(\alpha + \beta + \delta)](\alpha + \gamma)}{\sigma},$$

$$\omega_2^2 = \frac{\chi \varepsilon_w^0 (1 + \varepsilon_\rho)(\alpha + \gamma)}{\varepsilon_\rho}.$$
(21)

Based on the structure of our system, the following hypotheses can be established:

(H1) Transversality condition: Let $\kappa = (\kappa_1, \kappa_2)$ with $\kappa_1 := s$ and $\kappa_2 := \chi$, keeping all other parameters fixed. The squared frequencies depend affinely on (κ_1, κ_2) :

$$\begin{split} \omega_1^2(\kappa) &= \frac{\left(\kappa_1 - \sigma(\alpha + \beta + \delta)\right)\left(\alpha + \gamma\right)}{\sigma}, \\ \omega_2^2(\kappa) &= \frac{\kappa_2 \varepsilon_w^0 (1 + \varepsilon_\rho)(\alpha + \gamma)}{\varepsilon_\rho}. \end{split}$$

Hence, the crossing rates are:

$$\frac{\partial \omega_1^2}{\partial \kappa_1} = \frac{\alpha + \gamma}{\sigma} \neq 0, \qquad \frac{\partial \omega_2^2}{\partial \kappa_2} = \varepsilon_w^0(\alpha + \gamma) \frac{1 + \varepsilon_\rho}{\varepsilon_\rho} \neq 0,$$

so that:

$$\det \left(\frac{\partial(\omega_1^2, \omega_2^2)}{\partial(\kappa_1, \kappa_2)} \right) \bigg|_{(\kappa_1, \kappa_2) = (s, \chi)} \neq 0.$$

(H2) Non-resonance condition:

$$\sqrt{\frac{[s-\sigma(\alpha+\beta+\delta)](\alpha+\gamma)}{\sigma}} / \sqrt{\frac{\chi \varepsilon_w^0 (1+\varepsilon_\rho)(\alpha+\gamma)}{\varepsilon_\rho}} \neq \frac{m}{n}$$

where *m* and *n* are relatively prime, such that $m + n \le 5$.

(H3) Resonance condition:

$$\sqrt{\frac{[s-\sigma(\alpha+\beta+\delta)](\alpha+\gamma)}{\sigma}} / \sqrt{\frac{\chi \varepsilon_w^0 (1+\varepsilon_\rho)(\alpha+\gamma)}{\varepsilon_\rho}} = \frac{m}{n}$$

where m and n are relatively prime, such that $m + n \le 5$.

(H4) Eigenvalue assignment: If we assume that:

$$\sigma > 0$$
, $\alpha + \gamma > 0$, $s > \sigma(\alpha + \beta + \delta)$,

then the linearization of (19) at $\dot{\mathbf{X}}$ has two simple purely imaginary pairs

$$\lambda_{1,2} = \pm i\omega_1, \quad \lambda_{3,4} = \pm i\omega_2, \quad \text{with} \quad \omega_1, \, \omega_2 > 0.$$

Furthermore, let A denote the Jacobian matrix introduced in (20). From its characteristic polynomial we obtain

$$\det(\lambda I - A) = \lambda^4 + a_1 \lambda^3 + a_2 \lambda^2 + a_3 \lambda + a_4,$$

where the coefficients can be expressed, by means of the Newton identities in terms of the traces of powers of J, as follows:

$$\begin{split} a_1 &= -\operatorname{tr}(A) = 0, \\ a_2 &= \frac{1}{2} \left(\operatorname{tr}(A)^2 - \operatorname{tr}(A^2) \right) = (A_{12} A_{21} + A_{34} A_{43}), \\ a_3 &= -\frac{1}{6} \left(\operatorname{tr}(A)^3 - 3 \operatorname{tr}(A) \operatorname{tr}(A^2) + 2 \operatorname{tr}(A^3) \right) = 0, \\ a_4 &= \det(A) = A_{12} A_{21} A_{34} A_{43}. \end{split}$$

Next, we construct the Hurwitz principal minors:

$$\Delta_1 = a_1,$$

$$\Delta_2 = a_1 a_2 - a_3,$$

$$\Delta_3 = (a_1 a_2 - a_3) a_3 - a_1^2 a_4.$$

Therefore, we finally obtain $\Delta_3 = \Delta_1 = 0$.

Therefore, we have established the necessary and sufficient conditions for system (19) to undergo a **double Hopf bifurcation** at the equilibrium $\dot{\mathbf{X}}$, within the framework of Yu [40]; the same conclusion also follows from the generalization of Orlando's formula [41]. We now state this result formally in the following theorem.

Theorem 2. The non-resonant Hopf–Hopf bifurcation or resonant Hopf–Hopf bifurcation of system (19) occurs at $\dot{\mathbf{X}}$ if and only if the following conditions (H1), (H2) and (H4) or (H1), (H3) and (H4) hold.

Remark 1. The equilibrium is non-hyperbolic. In the absence of additional dissipative conditions, the generic Hopf–Hopf normal form yields oscillatory dynamics on the center manifold; hence the equilibrium is not locally asymptotically stable and, consequently, cannot be globally asymptotically stable. Moreover, Lyapunov stability cannot be certified via the direct method here, so to proceed one must instead use the normal-form (center-manifold) analysis.

Based on the results summarized in Theorem (2), we infer the coexistence and interaction of two endogenous cyclical mechanisms within the model proposed in this paper. The first cyclical mechanism is strongly associated with the interaction between the wage share (u) and the employment rate (v), as originally suggested by Goodwin [14]. This interpretation follows from the fact that the frequency ω_1 exactly matches the frequency obtained in the Goodwin model with capitalist savings and depreciation, as formulated in [38]. In particular, this frequency depends on the capitalist saving rate (s), which captures the intensity of capital accumulation and serves as the first bifurcation parameter in the transversality condition (H1). For this reason, we refer to this first cyclical mechanism as the *Goodwin cycle*,

The second cyclical mechanism can be interpreted as generated by an oscillatory relationship between the underemployment rate (z) and the type 2 relative wage (ε_w) . This interpretation follows from the structure of frequency ω_2 , which includes parameters that characterize the labor conditions of type 2 workers, such as their influence on the bargaining power of the working class (ε_p) , the equilibrium value of the type 2 relative wage (ε_w^0) , and the adjustment speed of underemployment (χ) , which serves as the second bifurcation parameter in (H1). Accordingly, we refer to this second cyclical mechanism as the *underemployment cycle*.

When the transversality condition (H1) and the non-resonance condition (H2) hold, the Goodwin cycle and the underemployment cycle operate at distinct frequencies. The coexistence of these two mechanisms gives rise to complex multi-periodic or quasi-periodic patterns, since both cycles persist but are not synchronized in time. In contrast, when the transversality condition (H1) and the resonance conditions (H3) are satisfied, both cyclical mechanisms become synchronized, implying that their oscillations occur in a fixed proportion over time. As a result, the Goodwin and underemployment cycles move in phase, producing stronger and more coherent fluctuations compared with the non-resonant case. Instead of complex multi-frequency patterns, single-frequency oscillations with amplified amplitude emerge.

Concerning Remark (1), it is important to note that due to the structure of the dynamical system, local stability conditions for the steady-state equilibrium cannot be established without the inclusion of nonlinear terms. Economically, this non-hyperbolic nature of the equilibrium implies that the system lacks intrinsic mechanisms of self-stabilization, leading the economy to fluctuate persistently around the steady state rather than converge to it.¹¹

5. Cubic Normal Form on the Center Manifold

Normal form analysis is a fundamental analytical methodology in bifurcation theory, serving a dual purpose: it furnishes a *robust* stability diagnosis while simultaneously informing the interpretation of numerical simulations. By reducing the system to its essential

¹¹This result suggests avenues for future research aimed at introducing additional stabilizing mechanisms, such as stronger labor-market institutions, government intervention, or external sector dynamics, that could render the steady-state equilibrium asymptotically stable.

dynamical structure, the signs of its coefficients (such as the terms P_{ii} derived below) analytically dictate whether local oscillations will amplify (instability) or attenuate (stability). Concurrently, this technique predicts the resultant dynamical morphology, accounting for the emergence of complex phenomena observed in simulations, such as quasi-periodic dynamics (dense tori) or phase-locking (resonance).

To compute the normal-form indices, we adopt the framework for non-resonant Hopf-Hopf bifurcation presented in [42, 43] and formalized in Theorem (2). The system (19) can be expressed as

$$\mathbf{X}' = F(\mathbf{X}, \kappa), \qquad \mathbf{X} \in \mathbb{R}^4, \ \kappa \in \mathbb{R}^2,$$
 (22)

which admits an equilibrium at $\dot{\mathbf{X}}$ for $\dot{\kappa} = (s, \chi)$. The Jacobian matrix A has two pairs of simple purely imaginary eigenvalues,

$$\lambda_{1,2} = \pm i\omega_1, \qquad \lambda_{3,4} = \pm i\omega_2, \qquad \omega_1, \omega_2 > 0.$$

Since these eigenvalues are simple, the corresponding eigenvectors $q_{1,2} \in \mathbb{C}^4$ satisfy $Aq_1 = i\omega_1 q_1$ and $Aq_2 = i\omega_2 q_2$. Explicitly,

$$q_1 = \begin{bmatrix} \frac{i \, \omega_1}{A_{21}} \\ 1 \\ 0 \\ 0 \end{bmatrix}, \quad q_2 = \begin{bmatrix} \frac{A_{13} A_{34} + i \omega_2 A_{14} + A_{12} A_{24}}{\omega_2^2 + A_{12} A_{21}} \\ \frac{-i A_{13} A_{21} A_{34} + \omega_2 A_{14} A_{21} + i \omega_2^2 A_{24}}{\omega_2 \left(\omega_2^2 + A_{12} A_{21}\right)} \\ \frac{A_{34}}{i \, \omega_2} \\ 1 \end{bmatrix}. \quad DH(\mathbf{0}) = Q \implies H_{w_1}(\mathbf{0}) = q_1, \quad H_{\overline{w_1}}(\mathbf{0}) = q_2, \quad H_{\overline{w_2}}(\mathbf{0}) = q_2, \quad H_{\overline{w_2}}(\mathbf{0$$

The adjoint eigenvectors $p_{1,2} \in \mathbb{C}^4$ satisfy $A^T p_1 = -i\omega_1 p_1$ and $A^{\mathsf{T}}p_2 = -i\omega_2 p_2$. Normalizing with respect to the standard scalar product, we impose

$$\langle p_1, q_1 \rangle = \langle p_2, q_2 \rangle = 1, \qquad \langle p_2, q_1 \rangle = \langle p_1, q_2 \rangle = 0.$$

Accordingly, we obtain

$$p_{1} = \begin{bmatrix} \frac{i \omega_{1}}{-2A_{12}} \\ \frac{1}{2} \\ \frac{\omega_{1} \left(\omega_{1} A_{13} + i A_{14} A_{43}\right) - A_{12} A_{24} A_{43}}{2A_{12} \left(\omega_{1}^{2} + \omega_{2}^{2}\right)} \\ \frac{\omega_{1} \left(i A_{13} A_{34} + \omega_{1} A_{14} + i A_{12} A_{24}\right)}{2A_{12} \left(\omega_{1}^{2} + \omega_{3}^{2}\right)} \end{bmatrix} \quad p_{2} = \begin{bmatrix} 0 \\ 0 \\ \frac{i \omega_{2}}{2A_{34}} \\ \frac{1}{2} \end{bmatrix}.$$

Let $T^c \subset \mathbb{R}^4$ denote the corresponding generalized critical eigenspace of A. The center manifold is parameterized by the complex amplitudes $\mathbf{W} = (w_1, w_2) \in \mathbb{C}^2$ via

$$\mathbf{X} - \dot{\mathbf{X}} = H(\mathbf{W}) := y, \qquad H : \mathbb{C}^2 \to \mathbb{R}^4.$$
 (23)

The dynamics restricted to the center manifold are given by

$$\mathbf{W}' = \frac{d\mathbf{W}}{dt} = G(\mathbf{W}), \qquad G: \mathbb{C}^2 \to \mathbb{C}^2. \tag{24}$$

Substituting (23) and (24) into (22) (evaluated at $\kappa = \dot{\kappa}$) yields the

$$DH(\mathbf{W}) G(\mathbf{W}) = F(\dot{\mathbf{X}} + H(\mathbf{W}), \dot{\kappa}) = F(\dot{\mathbf{X}} + y, \dot{\kappa}), \quad (25)$$

Hence, the homological equation (25) can be expressed as

$$H_{w_1} w'_1 + H_{\overline{w_1}} \overline{w}'_1 + H_{w_2} w'_2 + H_{\overline{w_2}} \overline{w}'_2 = F(\dot{\mathbf{X}} + y, \dot{\kappa}),$$
 (26)

where F admits the Taylor expansion

$$F\left(\dot{\mathbf{X}}+y,\dot{\kappa}\right) = A\,y + \frac{1}{2}B\left(y,y\right) + \frac{1}{6}C\left(y,y,y\right) + \cdots,$$

with

$$(B(\mathbf{a}, \mathbf{b}))_i = \sum_{j,k=1}^4 \frac{\partial^2 F_i}{\partial X_j \partial X_k} \bigg|_{(\check{\mathbf{X}},k)} a_j b_k,$$

$$(C(\mathbf{a}, \mathbf{b}, \mathbf{c}))_i = \sum_{j,k,n=1}^4 \frac{\partial^3 F_i}{\partial X_j \partial X_k \partial X_n} \bigg|_{(\check{\mathbf{X}},k)} a_j b_k c_n.$$

The dynamics of any vector $y \in T^c$ lying in the critical eigenspace

$$y = w_1 q_1 + \overline{w}_1 \overline{q}_1 + w_2 q_2 + \overline{w}_2 \overline{q}_2$$

with $w_1 = \langle p_1, y \rangle$ and $w_2 = \langle p_2, y \rangle$. Moreover, setting $P := \left[p_1^*, \overline{p}_1^*, p_2^*, \overline{p}_2^*\right]^{\mathsf{T}}$ with $p_i^* := \overline{p}_i^{\mathsf{T}}$ and $Q := \left[q_1, \overline{q}_1, q_2, \overline{q}_2\right]$, we write

$$PH(\mathbf{W}) = \begin{bmatrix} p_1^* \ y \\ \overline{p}_1 \ y \\ p_2^* \ y \\ \overline{p}_2 \ y \end{bmatrix} = \begin{bmatrix} \langle p_1, \ y \rangle \\ \langle \overline{p}_1, \ y \rangle \\ \langle p_2, \ y \rangle \\ \langle \overline{p}_2, \ y \rangle \end{bmatrix} = \begin{bmatrix} \overline{w}_1 \\ \overline{w}_1 \\ \underline{w}_2 \\ \overline{w}_2 \end{bmatrix} = \mathbf{W}.$$

Also, $PQ = \mathbb{I}$. Differentiating at W = 0 gives

$$P DH (\mathbf{0}) = D\mathbf{W}|_{\mathbf{W} = \mathbf{0}} \implies P DH (\mathbf{0}) = \mathbb{I}.$$

Because P sends each vector in the center subspace to its unique coordinates in the basis $\{q_1, \overline{q}_1, q_2, \overline{q}_2\}$, the coordinate map is bijective and hence invertible. Consequently,

$$DH\left(\mathbf{0}\right) = Q \quad \Longrightarrow \quad \begin{aligned} H_{w_{1}}(0) &= q_{1}, & H_{\overline{w}_{1}}(0) &= \overline{q}_{1}, \\ H_{w_{2}}(0) &= q_{2}, & H_{\overline{w}_{2}}(0) &= \overline{q}_{2}. \end{aligned}$$

$$H\left(\mathbf{W}\right) = \sum_{|\nu| \geq 1} \frac{1}{\nu!} h_{\nu} \mathbf{W}^{\nu}, \qquad G\left(\mathbf{W}\right) = \sum_{|\nu| \geq 1} \frac{1}{\nu!} g_{\nu} \mathbf{W}^{\nu},$$

$$H(\mathbf{W}) = w_1 q_1 + \overline{w}_1 \overline{q}_1 + w_2 q_2 + \overline{w}_2 \overline{q}_2$$

$$+ \sum_{\substack{j+k+n+m>0\\j \text{ } l}} \frac{1}{j! \ k! \ n! \ m!} \ h_{jknm} w_1^j \overline{w}_1^k w_2^n \overline{w}_2^m,$$

with $h_{jknm} \in \mathbb{C}^4$ and $h_{kjnm} = \overline{h}_{jknm}$. Collecting the coefficients of the $w_1^j \overline{w}_1^k w_2^n \overline{w}_2^m$ -terms with j + k + n + m = 2 in (26) gives

$$\begin{split} h_{1100} &= A^{-1}B\left(q_1,\overline{q}_1\right),\\ h_{2000} &= (2\mathrm{i}\omega_1I - A)^{-1}B\left(q_1,q_1\right),\\ h_{1010} &= [\mathrm{i}(\omega_1 + \omega_2)I - A]^{-1}B\left(q_1,q_2\right),\\ h_{1001} &= [\mathrm{i}(\omega_1 - \omega_2)I - A]^{-1}B\left(q_1,\overline{q}_2\right),\\ h_{0020} &= (2\mathrm{i}\omega_2I - A)^{-1}B\left(q_2,q_2\right),\\ h_{0200} &= (-2\mathrm{i}\omega_1I - A)^{-1}B\left(\overline{q}_1,\overline{q}_1\right),\\ h_{0011} &= A^{-1}B\left(q_2,\overline{q}_2\right),\\ h_{0110} &= [\mathrm{i}(\omega_2 - \omega_1)I - A]^{-1}B\left(\overline{q}_1,q_2\right). \end{split}$$

Collecting the coefficients of the resonant cubic terms in (26), one obtains the resonant cubic coefficients in the normal form

$$\begin{split} G_{2100} &= \left\langle p_1, C\left(q_1, q_1, \overline{q}_1\right) + B\left(h_{2000}, \overline{q}_1\right) + 2 \, B\left(h_{1100}, q_1\right) \right\rangle, \\ G_{1011} &= \left\langle p_1, C\left(q_1, q_2, \overline{q}_2\right) + B\left(h_{1010}, \overline{q}_2\right) + B\left(h_{1001}, q_2\right) \right. \\ &\quad + \left. B\left(h_{0011}, q_1\right) \right\rangle, \\ G_{1110} &= \left\langle p_2, C\left(q_1, \overline{q}_1, q_2\right) + B\left(h_{1100}, q_2\right) + B\left(h_{1010}, \overline{q}_1\right) \right. \\ &\quad + \left. B\left(h_{1001}, q_1\right) \right\rangle, \\ G_{0021} &= \left\langle p_2, C\left(q_2, q_2, \overline{q}_2\right) + B\left(h_{0020}, \overline{q}_2\right) + 2 \, B\left(h_{0011}, q_2\right) \right\rangle, \end{split}$$

and the corresponding cubic coefficients h_{jknm} satisfying the orthogonality conditions:

$$\begin{split} h_{2100} &= (i\omega_1 I_n - A)^{-1} \left[C \left(q_1, q_1, \overline{q}_1 \right) + B \left(h_{2000}, \overline{q}_1 \right) \right. \\ &+ 2 \left. B \left(h_{1100}, q_1 \right) - G_{2100} \left. q_1 \right], \\ h_{1011} &= (i\omega_1 I_n - A)^{-1} \left[C \left(q_1, q_2, \overline{q}_2 \right) + B \left(h_{1010}, \overline{q}_2 \right) + B \left(h_{1001}, q_2 \right) \right. \\ &+ \left. B \left(h_{0011}, q_1 \right) - G_{1011} \left. q_1 \right], \\ h_{1110} &= (i\omega_2 I_n - A)^{-1} \left[C \left(q_1, \overline{q}_1, q_2 \right) + B \left(h_{1100}, q_2 \right) \right. \\ &+ \left. B \left(h_{1010}, \overline{q}_1 \right) + B \left(\overline{h}_{1001}, q_1 \right) - G_{1110} \left. q_2 \right], \\ h_{0021} &= (i\omega_2 I_n - A)^{-1} \left[C \left(q_2, q_2, \overline{q}_2 \right) + B \left(h_{0020}, \overline{q}_2 \right) \right. \\ &+ 2 \left. B \left(h_{0011}, q_2 \right) - G_{0021} \left. q_2 \right]. \end{split}$$

Then, the system (22) restricted to the center manifold takes the

α	β	δ	S	σ	γ	ε_a	ε_p	ϵ_w^0	ρ	u_0	v_0	z_0	$\epsilon_{w,0}$	ω_1
0.016	0.016	0.052	0.61	2.725	0.227	0.7	0.7	0.7	0.625	0.6	0.95	0.6	0.65	0.184348

Table 1
Parameter values, initial conditions, and frequency of the Goodwin cycle for system (19).

normal form

$$w'_{1} = i\omega_{1}w_{1} + \frac{1}{2}G_{2100}w_{1}|w_{1}|^{2} + G_{1011}w_{1}|w_{2}|^{2} + O(\|(w_{1}, w_{2})\|^{5}),$$

$$w'_{2} = i\omega_{2}w_{2} + G_{1110}w_{2}|w_{1}|^{2} + \frac{1}{2}G_{0021}w_{2}|w_{2}|^{2} + O(\|(w_{1}, w_{2})\|^{5}).$$
(27)

Moreover, if

$$(\text{Re }G_{2100}) (\text{Re }G_{1011}) (\text{Re }G_{1110}) (\text{Re }G_{0021}) \neq 0,$$

the system (22) is locally smoothly orbitally equivalent near the bifurcation to

$$\begin{split} v_{1}' &= v_{1} \left(\frac{1}{2} P_{11} \left| v_{1} \right|^{2} + P_{12} \left| v_{2} \right|^{2} \right) + O \left(\left\| \left(v_{1}, v_{2} \right) \right\|^{5} \right), \\ v_{2}' &= v_{2} \left(P_{21} \left| v_{1} \right|^{2} + \frac{1}{2} P_{22} \left| v_{2} \right|^{2} \right) + O \left(\left\| \left(v_{1}, v_{2} \right) \right\|^{5} \right). \end{split}$$

with

$$P_{11} = \text{Re } G_{2100},$$
 $P_{12} = \text{Re } G_{1011},$
 $P_{21} = \text{Re } G_{1110},$ $P_{22} = \text{Re } G_{0021}.$

Let $v_1=r_1e^{i\varphi_1}$ and $v_2=r_2e^{i\varphi_2}$, in polar coordinates $(r_1,r_2,\varphi_1,\varphi_2)$, the system before can be written as:

$$\begin{split} r_1' &= r_1 \Big(\frac{1}{2} \, P_{11} \, r_1^2 + P_{12} \, r_2^2 \Big) + + O \left(\parallel \left(r_1, r_2 \right) \parallel^5 \right), \\ r_2' &= r_2 \Big(P_{21} \, r_1^2 + \frac{1}{2} \, P_{22} \, r_2^2 \Big) + O \left(\parallel \left(r_1, r_2 \right) \parallel^5 \right), \\ \varphi_1' &= \omega_1 + \frac{1}{2} \, \operatorname{Im} G_{2100} \, r_1^2 + \operatorname{Im} G_{1011} \, r_2^2 + \Psi_1(r_1, r_2, \varphi_1, \varphi_2), \\ \varphi_2' &= \omega_2 + \operatorname{Im} G_{1110} \, r_1^2 + \frac{1}{2} \, \operatorname{Im} G_{0021} \, r_2^2 + \Psi_2(r_1, r_2, \varphi_1, \varphi_2). \end{split}$$

with Ψ_k is a smooth remainder in the phase equations that is 2π periodic in each angle and vanishes with the amplitudes.

Now, in examining the resonance cases associated with the double Hopf bifurcation [44, 43], and following the detailed analyses of the specific resonance conditions 1:1, 1:2, and 1:3 presented in [45, 46, 47, 48], we employ the coefficients of the resonant cubic terms G_{jknm} to construct the corresponding normal forms for each resonance case described in Theorem (2). Accordingly, the following specific formulations from (27) are obtained:

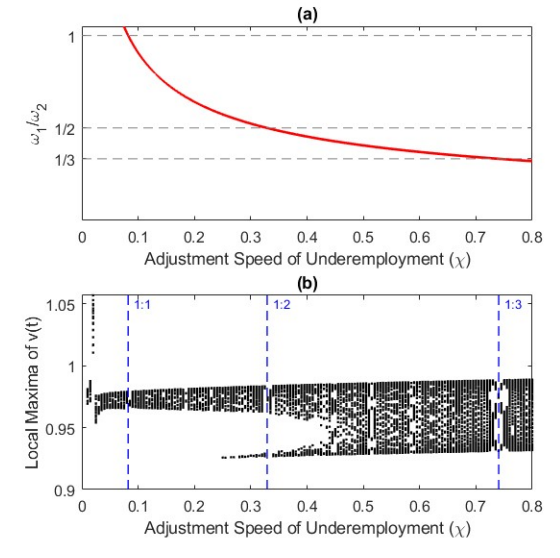


Figure 1: (a) Theoretical frequency ratio ω_1/ω_2 as a function of the adjustment speed of underemployment, χ . (b) Numerical bifurcation diagram for the local maxima of the employment rate.

• 1:1 **resonance** ($\omega_1 = \omega_2 = \omega$). The normal form takes the structure

$$\begin{split} w_1' &= i\omega\,w_1 + \frac{1}{2}G_{2100}\,w_1|w_1|^2 + G_{1011}\,w_1|w_2|^2 \\ &+ G_1\,\overline{w}_1w_2^2 + O\left(\left\|(w_1,w_2)\right\|^4\right), \\ w_2' &= i\omega\,w_2 + G_{1110}\,w_2|w_1|^2 + \frac{1}{2}G_{0021}\,w_2|w_2|^2 \\ &+ G_2\,w_1^2\overline{w}_2 + O\left(\left\|(w_1,w_2)\right\|^4\right), \end{split}$$

where the remainder is $O(\|(w_1, w_2)\|^4)$ due to the presence of the quadratic resonant monomials $(\overline{w}_1 w_2^2, w_1^2 \overline{w}_2)$. Consequently,

$$\begin{split} G_1 &= \left\langle p_1, C\left(\overline{q}_1, q_2, q_2\right) + 2B\left(h_{0110}, q_2\right) + B\left(h_{0020}, \overline{q}_1\right)\right\rangle, \\ G_2 &= \left\langle p_2, C\left(q_1, q_1, \overline{q}_2\right) + B\left(h_{2000}, \overline{q}_2\right) + 2B\left(h_{1001}, q_1\right)\right\rangle. \end{split}$$

• 1:2 **resonance** ($\omega_2 = 2\omega_1$). In this case the normal form is

$$\begin{split} w_1' &= i\omega_1 w_1 + \frac{1}{2} G_{2100} w_1 |w_1|^2 + G_{1011} w_1 |w_2|^2 \\ &+ G_1 \overline{w}_1 w_2 + O\left(\|(w_1, w_2)\|^3\right), \\ w_2' &= i\omega_2 w_2 + G_{1110} w_2 |w_1|^2 + \frac{1}{2} G_{0021} w_2 |w_2|^2 \\ &+ G_2 w_1^2 + O\left(\|(w_1, w_2)\|^3\right), \end{split}$$

with $O(\|(w_1,w_2)\|^3)$ arising from the quadratic resonant monomials $(\overline{w}_1w_2,w_1^2)$. Therefore,

$$G_{1}=\left\langle p_{1},\;B\left(\overline{q}_{1},q_{2}\right)\right\rangle ,\qquad G_{2}=\frac{1}{2}\left\langle p_{2},\;B\left(q_{1},q_{1}\right)\right\rangle .$$

• 1:3 **resonance** ($\omega_2 = 3\omega_1$). The corresponding normal form is

$$\begin{split} w_1' &= i\omega_1 w_1 + \frac{1}{2} G_{2100} w_1 |w_1|^2 + G_{1011} w_1 |w_2|^2 \\ &+ G_1 \overline{w}_1^2 w_2 + O\left(\|(w_1, w_2)\|^4\right), \\ w_2' &= i\omega_2 w_2 + G_{1110} w_2 |w_1|^2 + \frac{1}{2} G_{0021} w_2 |w_2|^2 \\ &+ G_2 w_1^3 + O\left(\|(w_1, w_2)\|^4\right), \end{split}$$

where the order $O(\|(w_1, w_2)\|^4)$ reflects the quadratic resonant monomials $(\overline{w}_2 w_1^2, w_1^3)$. Hence,

$$\begin{split} G_1 &= \left\langle p_1, C\left(\overline{q}_1, \overline{q}_1, q_2\right) + B\left(h_{0200}, q_2\right) + 2B\left(h_{0110}, \overline{q}_1\right)\right\rangle, \\ G_2 &= \left\langle p_2, C\left(q_1, q_1, q_1\right) + 3B\left(h_{2000}, q_1\right)\right\rangle. \end{split}$$

6. Numerical Simulations

To illustrate the dynamics of the system and compute the coefficients of the cubic normal form, we conducted numerical simulations. All simulations were performed in Matlab (R2024b) using ode45 with relative tolerance 10^{-6} and absolute tolerance 10^{-8} . The vector field is evaluated from the symbolic specification in Section 2 to ensure consistent Jacobians for variational computations (normal-form indices). The bifurcation package MatCont [49, 50] was used *only* as an exploratory tool to locate parameter regions of interest and to cross-check resonance locations.

Concerning parameter values, we adopt the estimates of α , β , δ , s, σ and γ for the U.S. economy reported in [38]. For type 2 relative productivity ε_a , type 2 relative bargaining power ε_p , and the equilibrium value of the type 2 relative wage ε_w^0 , we set all three equal to 0.7, representing an empirically plausible asymmetry between type 1 and type 2 workers. ¹². Given these parameter values, we use equation (18)

¹²Under this configuration, type 2 workers are assumed to be 70% as productive as type 1 workers; their influence on the growth rate of real wages is 70% of that of type 1 workers; and their equilibrium relative wage corresponds to 70% of the wage level of type 1 workers.

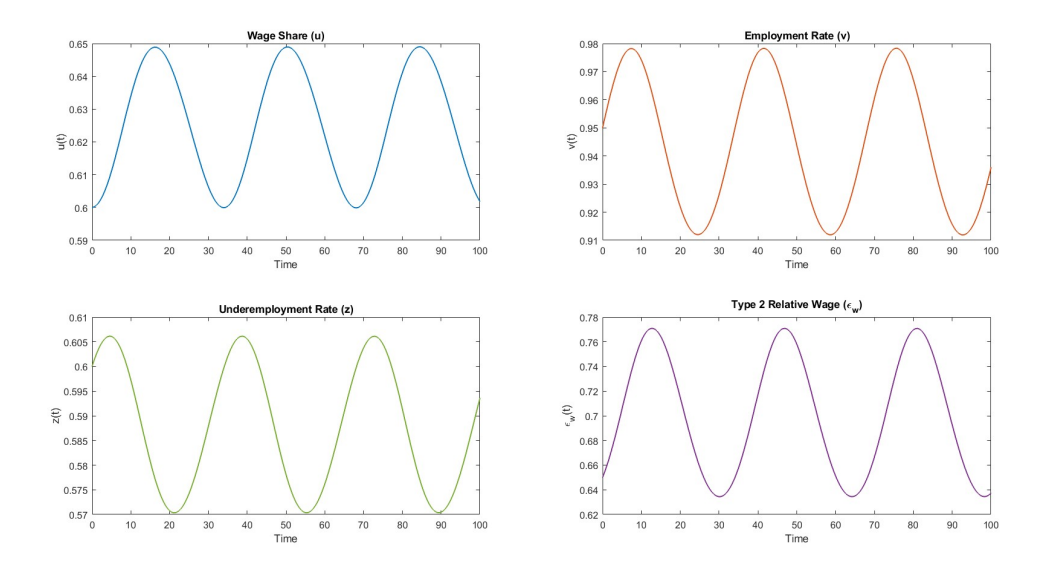


Figure 2: Time series evolution of the state variables for the 1:1 resonance case ($\chi \approx 0.08227$).

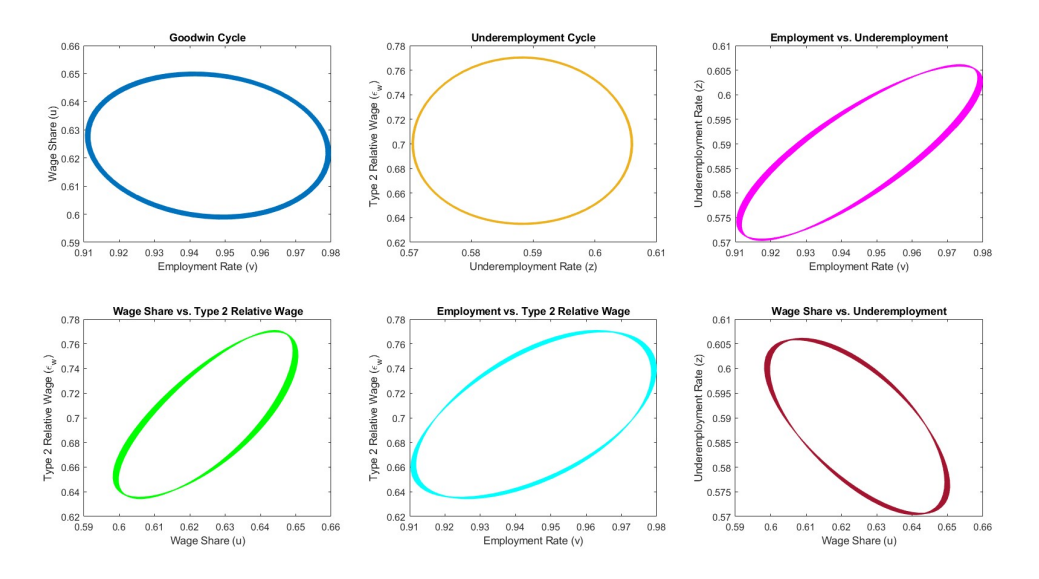


Figure 3: Comprehensive 2D phase portraits for the 1:1 resonance case ($\chi \approx 0.08227$).

to calibrate ρ so that the equilibrium employment rate \dot{v} matches the value reported in [38]. This parameterization yields a frequency for the Goodwin cycle of $\omega_1=0.184348394$. The term χ is treated as a free calibration parameter that allows us to vary the frequency of the underemployment cycle, ω_2 , and thereby explore alternative dynamic regimes of the model.

The initial conditions for the state variables $(u_0,v_0,z_0,\varepsilon_{w,0})$ are chosen as a representative point in the state space, located in close proximity to the non-trivial equilibrium. This selection ensures that the initial state lies within the basin of attraction of the stable limit cycle generated by the double Hopf bifurcation. Such an initialization enables the simulation to illustrate the tendency of the system to converge toward its characteristic quasi-periodic attractor. The corresponding parameter values, initial conditions, and frequency of the Goodwin cycle are summarized in Table (1).

Figure (1) summarizes the response of the dynamical system to variations in the adjustment speed of underemployment, χ . Panel (a) depicts the theoretical frequency ratio ω_1/ω_2 as a function of χ , allowing the identification of the resonant cases at 1.000021 ($\chi=0.08227$), 1.999981 ($\chi=0.32906$), and 2.999981 ($\chi=0.74039$). For illustrative purposes, two non-resonant cases are also

selected: $1.3333 \approx 4/3$ ($\chi = 0.14625$), which approximates a rational frequency ratio, and $1.4142 \approx \sqrt{2}$ ($\chi = 0.16453$), which approximates an irrational ratio. These values are consistent with the affine dependence of the squared frequencies derived in Eq. (21) and confirm the transversality condition (H1) stated in Theorem (2).

Panel (b) presents the numerical bifurcation diagram for the local maxima of the employment rate, illustrating how variations in χ affect the long-run dynamics of the system. The diagram reveals alternating regions of ordered and complex behavior. Narrow periodic windows appear near the resonant frequency ratios, indicating regular, synchronized cycles in which the employment rate follows a predictable sequence of maxima. Between these resonant windows, the plot becomes densely populated, reflecting complex quasi-periodic motion in which the maxima of v no longer repeat exactly. As the adjustment speed of underemployment (χ) increases, the diagram becomes progressively more intricate, suggesting that the system transitions toward increasingly irregular oscillations through successive resonances. Given $\omega_1 = 0.184348394$, the corresponding periods for the resonant cases are $T_1 \approx 34.09$ (1:1), $T_2 \approx 17.04$ (1:2), and $T_3 \approx 11.36$ (1:3), which match the observed spacing of the maxima. This structure constitutes the numerical counterpart of the

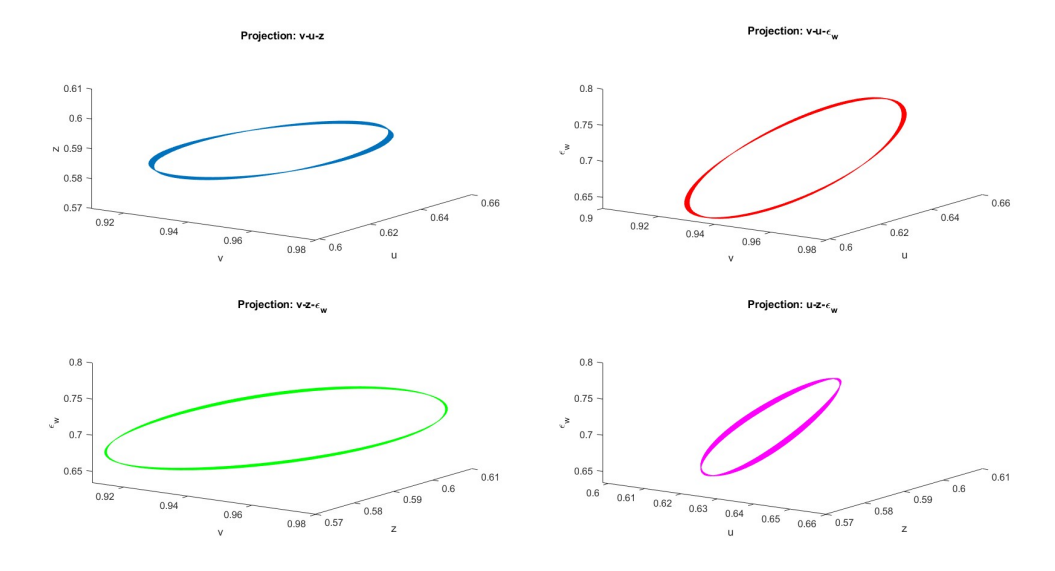


Figure 4: Comprehensive 3D projections of the system attractor for the 1:1 resonance case ($\chi \approx 0.08227$).

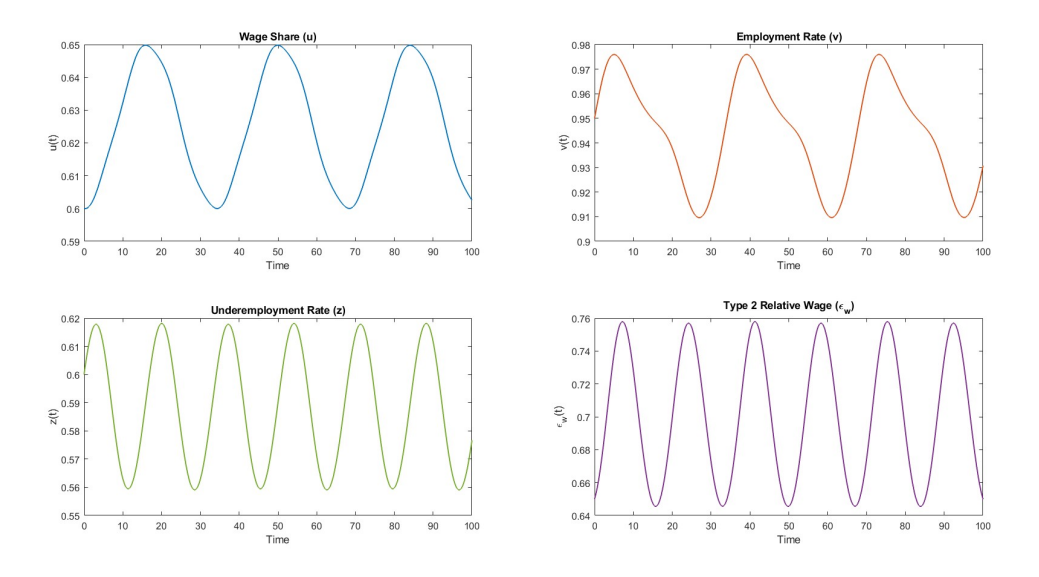


Figure 5: Time series evolution of the state variables for the 1:2 resonance case ($\chi \approx 0.32906$).

center-manifold normal form analyzed in Section 5 and reproduces the resonance patterns discussed after Eq. (27).

6.1. Dynamics under the 1:1 resonant Hopf-Hopf bifurcation

This subsection discusses the behavior of the system under a 1:1 resonance condition, which occurs when the frequencies of the Goodwin and underemployment cycles are equal ($\omega_1=\omega_2$). For this simulation, the speed of adjustment of underemployment is set to $\chi\approx 0.08227$. The cubic coefficients and the resonant quadratics are reported below:

 $\begin{aligned} G_{2100} &= 0.107163 \text{ i}, \\ G_{1011} &= 0.026209 + 0.019883 \text{ i}, \\ G_{1110} &= -0.078294 \text{ i}, \\ G_{0021} &= -0.115613 + 0.061771 \text{ i}, \end{aligned}$

with the resonant terms:

$$G_1 = 0.214336 + 0.244343 i,$$
 $G_2 = -0.051601 - 0.195733 i.$

The time series in Fig. (2) exhibit near-sinusoidal, phase-locked oscillations with $\omega_1=\omega_2=0.184348394$. The amplitudes evolve under $P_{11}\approx 0$, $P_{12}=0.026209$, $P_{21}\approx 0$ and $P_{22}=-0.115613$: the Goodwin pair grows solely through cross-coupling from the underemployment pair, while the latter self-saturates. This mechanism

accounts for the single-tone envelopes observed in u,v,z,ε_w at the period $T\approx 34.08$. All four state variables move in perfect synchrony, completing their cycles over the same period. The oscillations are stable, with u moving from 0.60 up to 0.65, while v cycles between 0.91 and 0.98. z shows a tight oscillation, fluctuating from 0.575 up to 0.605, and ε_w shows a wide amplitude, moving from a low of 0.64 up to 0.76.

In Fig. (3), the (u,v) cycle traces a simple, stable ellipse, and the (z,ϵ_w) cycle also forms a clean ellipse, with its shape defined by the ϵ_w oscillation reaching 0.76. Furthermore, Fig. (4) also confirms, through the ellipses in (u,v) and (z,ϵ_w) , the presence of a single closed orbit, corresponding to a torus collapsed by the 1:1 locking. With $P_{12}>0$ and $P_{22}<0$, the amplitude flow governed by Eq. (27) again selects a mixed-mode cycle in which the underemployment block stabilizes the nonlinear dynamics while simultaneously feeding the Goodwin block. This configuration remains consistent with the 1:1 reduced system.

6.2. Dynamics under the 1:2 resonant Hopf-Hopf bifurcation

Here, we analyze the dynamics under a 1:2 resonance, where the frequency of the underemployment cycle is twice that of the Goodwin cycle ($\omega_2 = 2\omega_1$). This case is simulated by setting the adjustment

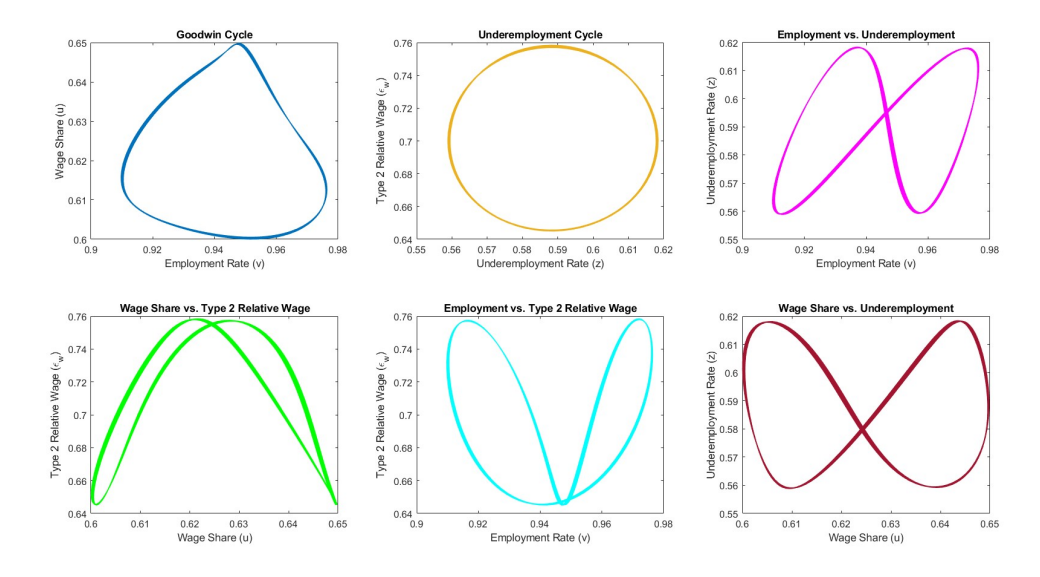


Figure 6: Comprehensive 2D phase portraits for the 1:2 resonance case ($\chi \approx 0.32906$).

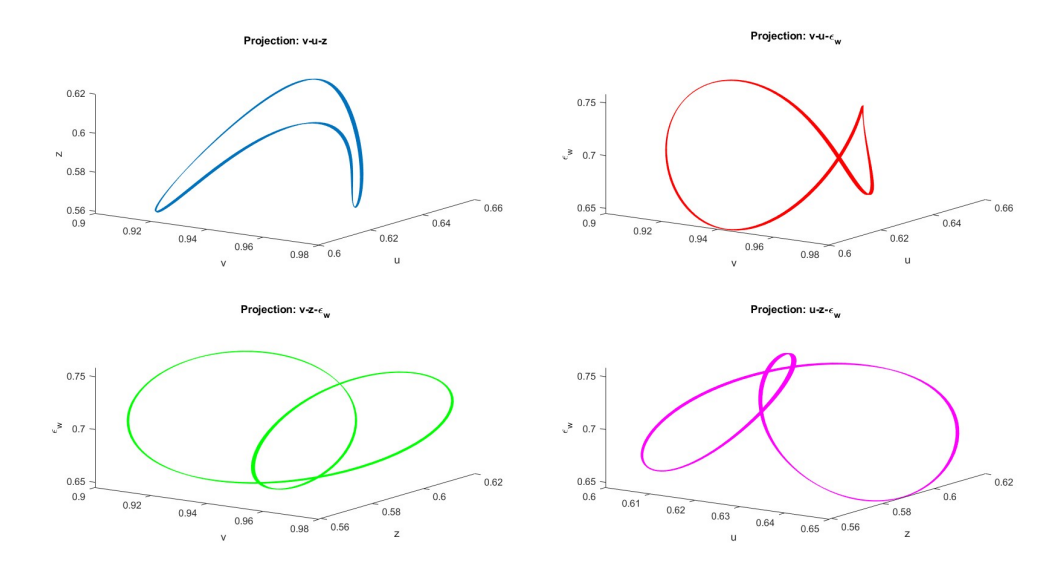


Figure 7: Comprehensive 3D projections of the system attractor for the 1:2 resonance case ($\chi \approx 0.32906$).

speed of underemployment to $\chi \approx 0.32906$. The coefficients computed below exhibit a single nonzero quadratic resonance:

$$\begin{split} G_{2100} &= 0.107163 \, \mathrm{i}, \\ G_{1011} &= 0.028133 + 0.021342 \, \mathrm{i}, \\ G_{1110} &= -0.250529 \, \mathrm{i}, \\ G_{0021} &= -0.322539 + 0.008230 \, \mathrm{i}, \end{split}$$

with the resonant terms:

$$G_1 = 0.030824, \qquad G_2 = 0.$$

From the time series exhibit in Fig. (5), the variables z and ε_w oscillate at twice the frequency, completing two full sinusoidal waves in the same time it takes u and v to complete one cycle. This 1:2: $\omega_2=0.368693214\approx 2\omega_1$ and $T_2\approx 17.04$ coupling alters the slow dynamics, inducing a "tall/short" peak pattern in v and u, where major peaks reach 0.65 while minor peaks are limited to 0.63. The amplitude coefficients $P_{12}=0.028133$ and $P_{22}=-0.322539$ once again yield cross-feeding from the fast block to the slow one, with self-limitation in the fast block. So the visible morphology is dictated by the amplitude block— $P_{12}>0$ and $P_{22}<0$ —already reflected in the alternating tall/short peaks of u.

In Fig. (6), the dynamics is strictly 1:2 phase–locked: the closed traces show no beat or envelope drift over multiple laps, and the spectrum contains only $(\omega_1, 2\omega_1)$ without sidebands above numerical noise. The two lobes in mixed projections have near-equal area and uniform arc–length density, indicating negligible slow–amplitude variation along the orbit. Now, we observe that the $(z-\epsilon_w)$ projection remains a clean ellipse (see Figs. (9), (11), and (13)), as it represents the self-limited ω_2 fast–oscillating mode (consistent with $P_{22} < 0$), which serves as the source of the second frequency.

In contrast, the (u-v) cycle is warped, as the slow ω_1 mode is forced by the $2\times$ frequency. Critically, mixed projections plotting a $1\times$ variable (like v) against a $2\times$ variable (like z) must trace two excursions of the fast variable for every one of the slow. This creates the geometric manifestation of the 1:2 resonance: a two-lobed, "figure-eight" motif, as seen in (v-z), where z cycles from 0.55 to 0.62. The 3D views in Fig. (7) display a single smooth closed orbit; the apparent constriction is a rendering/projection artifact rather than a genuine pinch. The orbit closes after two excursions of the fast variables for each slow cycle, consistent with 1:2 phase locking.

6.3. Dynamics under the 1:3 resonant Hopf-Hopf bifurcation

This subsection explores the 1:3 resonance condition, where the frequency of the underemployment cycle is three times that of the

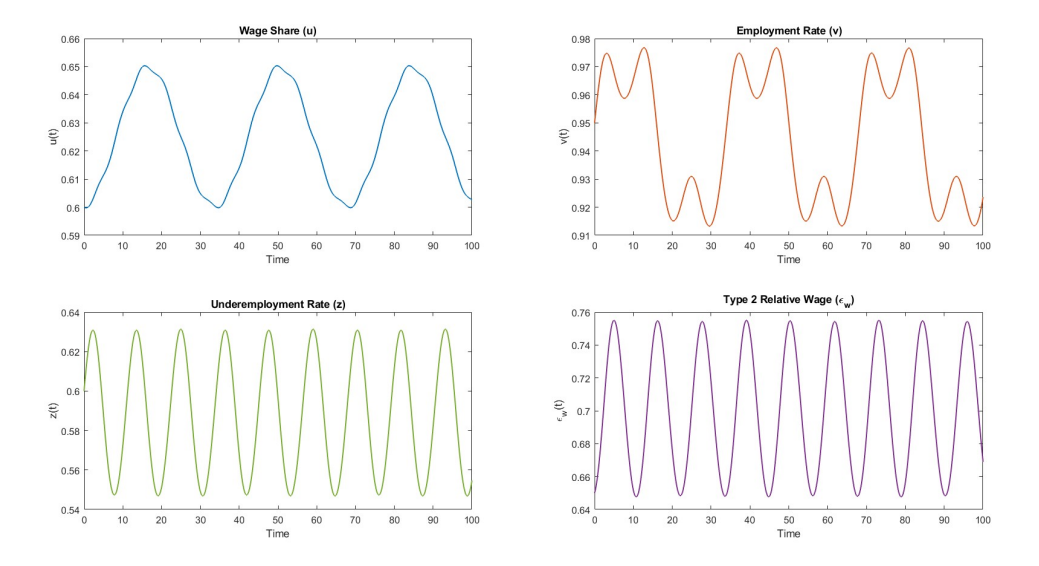


Figure 8: Time series evolution of the state variables for the 1:3 resonance case ($\chi \approx 0.74039$).

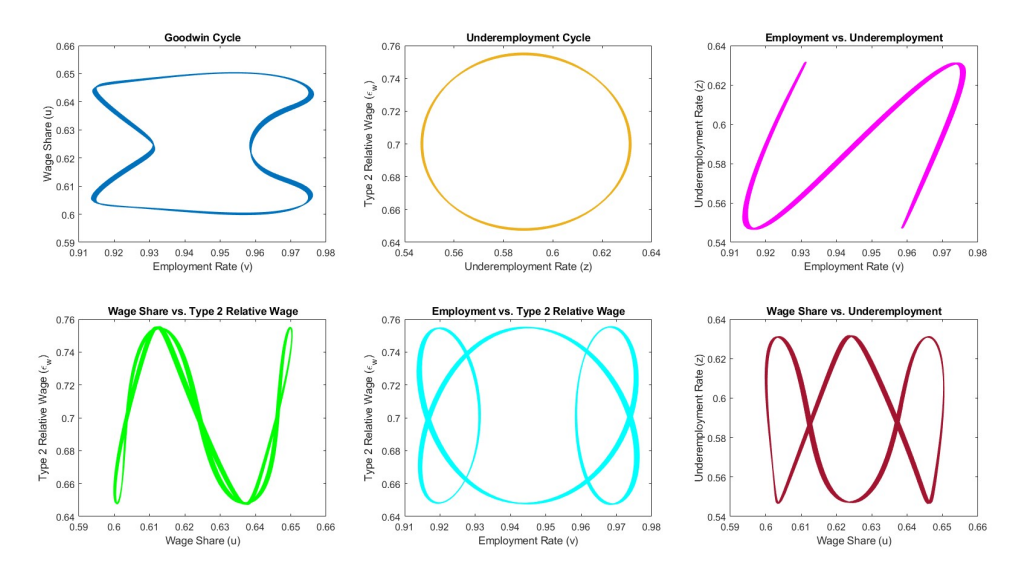


Figure 9: Comprehensive 2D phase portraits for the 1:3 resonance case ($\chi \approx 0.74039$).

Goodwin cycle ($\omega_2 = 3\omega_1$). The simulation is conducted with an adjustment speed of underemployment of $\chi \approx 0.74039$. As detailed below, the quadratic term exerts a significant influence:

$$\begin{split} G_{2100} &= 0.107163 \text{ i}, \\ G_{1011} &= 0.034452 + 0.026136 \text{ i}, \\ G_{1110} &= -0.543561 \text{ i}, \\ G_{0021} &= -0.546163 - 0.190480 \text{ i}, \end{split}$$

with resonant terms:

$$G_1 = -0.051896 - 0.085510 i, G_2 = 0.$$

In Fig. (8) we note that the series show tripling of the fast block: $\omega_2 = 0.553041688 \approx 3\omega_1$ with $T_2 \approx 11.36$. The fast variables z and ϵ_w complete three oscillations, with ϵ_w moving from 0.65 to 0.75, for every single slow cycle of u, which goes from 0.60 to 0.65. As noted, v now shows highly considerable changes; the injection of a strong third harmonic from the fast cycle induces a much more complex and pronounced modulation on the v waveform than in the 1:2 case. Amplitude flow is weaker but of the same sign pattern as above ($P_{12} = 0.034452$, $P_{22} = -0.546163$), so the Goodwin pair remains slaved to the underemployment pair for amplitude selection while the fast block self-limits. At the reported amplitudes, the visible morphology

is set by the amplitude coefficients— $P_{12} > 0$ and $P_{22} < 0$ —so the fast block self-limits while cross–feeding the slow one.

For Fig. (9), the mixed planes show the canonical three–lobed motifs and an S–shaped loop in (u,v), consistent with 1:3 phase locking (three excursions of (z, ε_w) per slow cycle). Hence the lobes are most prominent in projections involving ε_w . In Fig. (10), the closed traces complete three wraps in the fast coordinates per one slow rotation, matching the 1:3 winding. The observed twisting and sharper features follow from the tri–lobed geometry and modal participation under the 1:3 coupling, not from additional slow modulation. No thickening is visible, indicating absence of slow drift; this is consistent with exact locking at $\omega_2/\omega_1 \approx 3$ and the presence of the 1:3 resonant monomials listed after Eq. (27).

6.4. Dynamics under non-resonant conditions

To contrast with the resonant cases, we also explore the dynamics of the system when the frequency ratio is not a simple integer ratio.

6.4.1. Rational frequency ratio

First, we consider a non-resonant case in which the frequency ratio is a more complex rational number, specifically $\omega_1/\omega_2 = 3/4$. This scenario is simulated using $\chi \approx 0.14625$. The coefficients below describe the generic double–Hopf coupling without quadratic

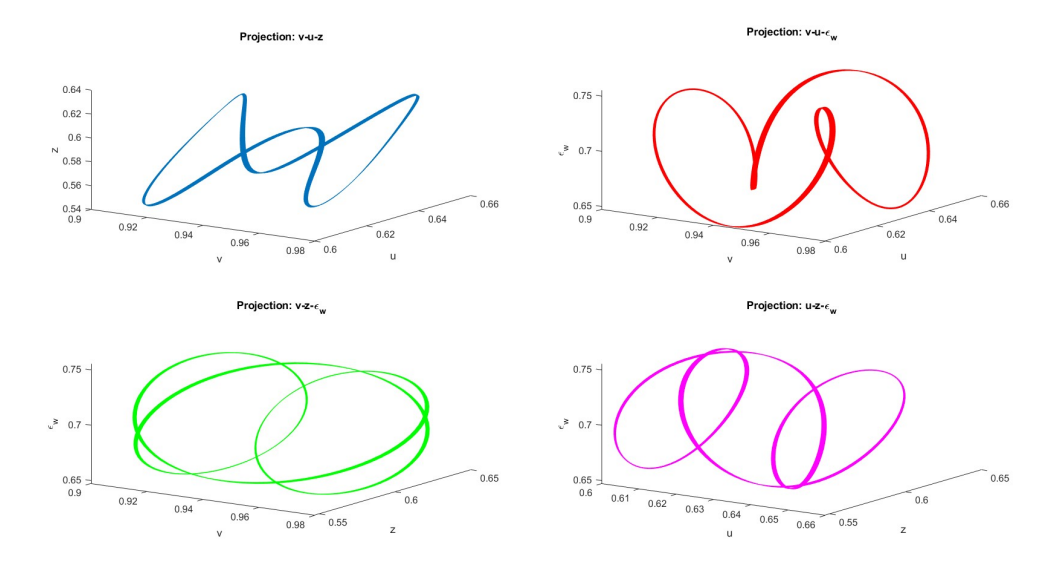


Figure 10: Comprehensive 3D projections of the system attractor for the 1:3 resonance case ($\chi \approx 0.74039$).

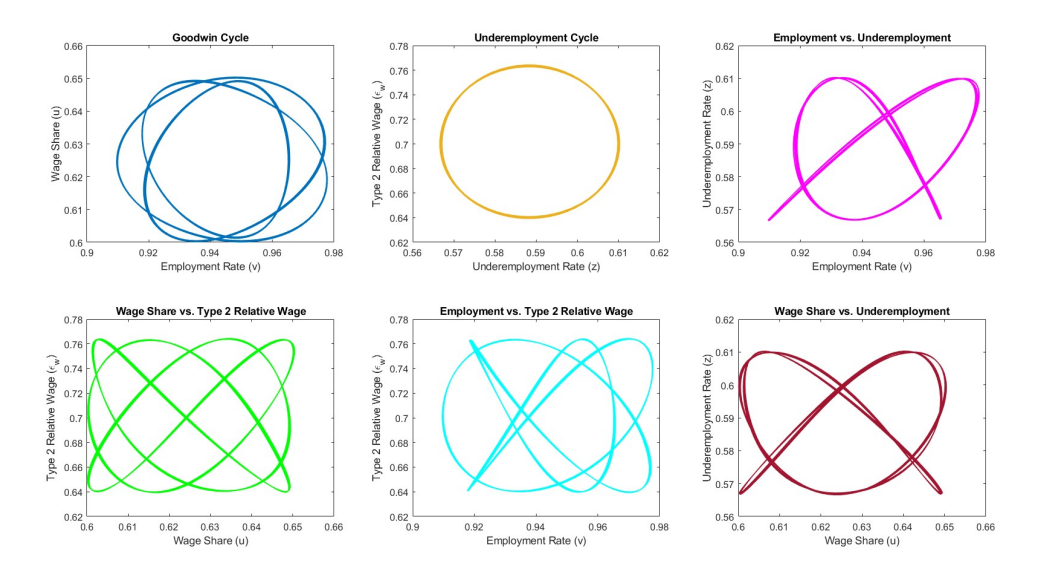


Figure 11: Comprehensive 2D phase portraits for the non resonance case but with rational ratio ($\chi \approx 0.14625$).

resonant terms:

$$\begin{split} G_{2100} &= 0.107163 \text{ i}, \\ G_{1011} &= 0.025205 + 0.019122 \text{ i}, \\ G_{1110} &= -0.121469 \text{ i}, \\ G_{0021} &= -0.175761 + 0.062620 \text{ i}. \end{split}$$

In Fig. (11), the (u,v) and $v-\epsilon_w$ panels show rosette–like closures with three and four petals, respectively, consistent with the 3:4 winding dictated by the measured frequencies. The "underemployment circle" remains nearly round, reflecting modest deformation in (z,ϵ_w) . Because the ratio is rational but nonresonant (no quadratic resonance terms), the center–manifold dynamics yields a periodic orbit (a closed trajectory) on the invariant two–torus rather than quasi–periodic filling. The frequencies share a common multiple. The system is therefore periodic, and the attractor is a complex, one–dimensional closed curve. This is observed in the "rosette-like" closures of Fig. (11): the $(v-\epsilon_w)$ projection forms a four-petaled figure (with ϵ_w oscillating from 0.64 to 0.76), while (v-z) shows three petals (with z moving from 0.57 to 0.61).

In Fig. (12), the 3D projections show a single closed space curve that wraps several times around the fast directions before returning to its starting point after the common period (about 102 in our run).

The petal count and their placement reflect the 3:4 winding (three slow rotations per four fast excursions), i.e., periodic closure on the invariant two–torus rather than quasiperiodic filling. Consistent with the amplitude block, $P_{12} > 0$ and $P_{22} < 0$, the oscillations remain bounded and the tube thickness is nearly uniform along the orbit. Any visible twisting is mild and attributable to the 3:4 geometry and projection, not to additional resonant forcing.

6.4.2. Irrational frequency ratio

Finally, we examine a case in which the frequency ratio is irrational, leading to quasi-periodic motion on the surface of a torus. For this simulation, we set the ratio $\omega_1/\omega_2=1/\sqrt{2}$ by choosing $\chi\approx 0.16453$. The coefficients listed below specify the nonresonant normal form:

$$\begin{split} G_{2100} &= 0.107163 \, \mathrm{i}, \\ G_{1011} &= 0.025366 + 0.019243 \, \mathrm{i}, \\ G_{1110} &= -0.134212 \, \mathrm{i}, \\ G_{0021} &= -0.192226 + 0.059917 \, \mathrm{i}. \end{split}$$

In Fig. (13), each 2D panel shows a densely filled band—the planar trace of quasi-periodic motion on an invariant two-torus—rather than a single closed loop. With $\omega_2/\omega_1 \approx \sqrt{2}$, the mixed projections (e.g., v versus ε_w) tile the plane in a nearly rectangular pattern, as

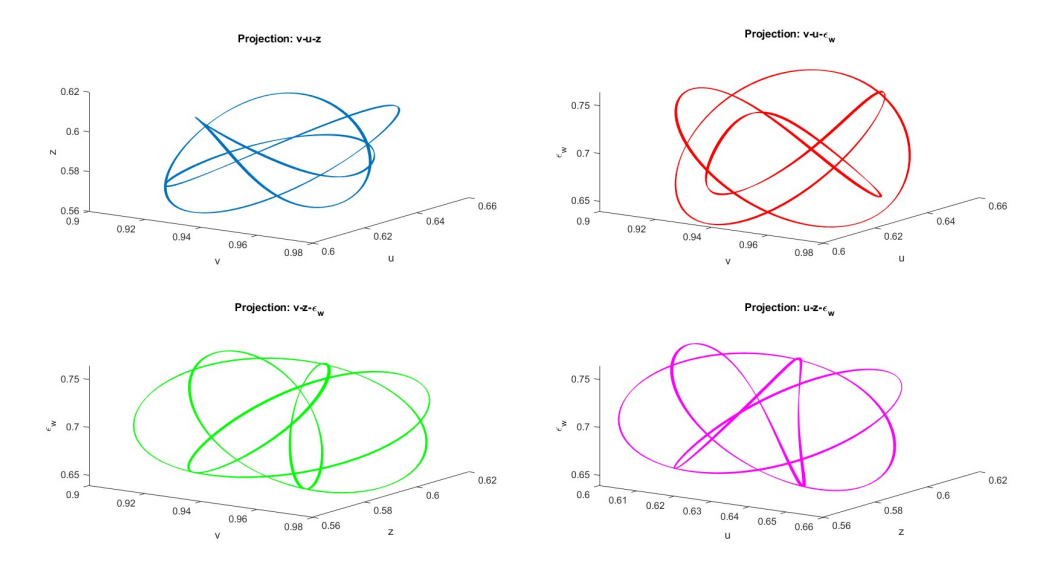


Figure 12: Comprehensive 3D projections of the system attractor for the non resonance case but with rational ratio ($\chi \approx 0.14625$).

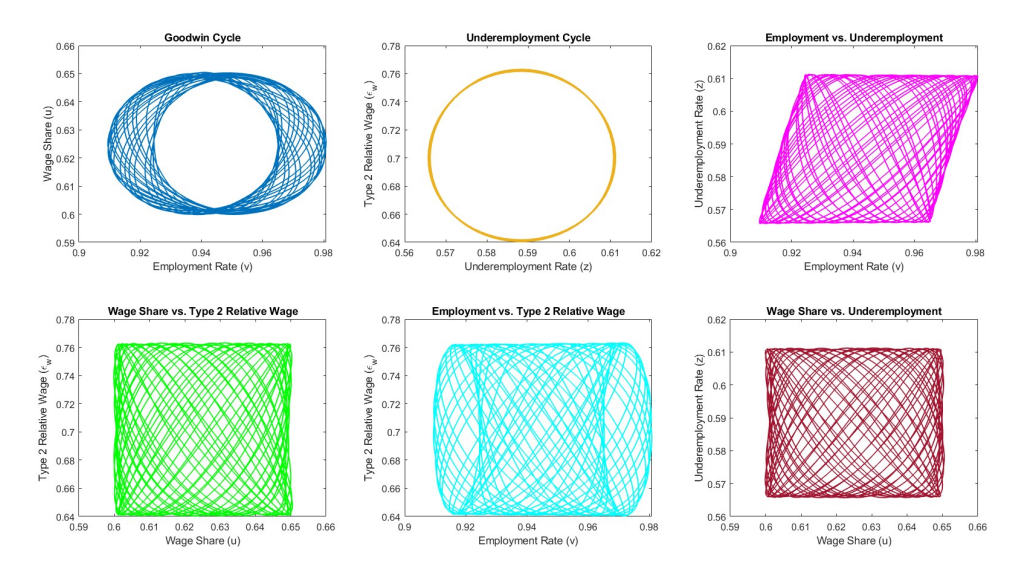


Figure 13: Comprehensive 2D phase portraits for the non resonance case but with irrational ratio ($\chi \approx 0.16453$).

expected for an irrational rotation. The amplitude dynamics keeps the tube thickness essentially uniform across traversals and the frequencies *never* share a common multiple. The system is *quasi-periodic*. The trajectory never closes and, over time, passes arbitrarily close to every point on a two–dimensional surface.

Thus, the attractor is the "filled two-torus" seen in Fig. (14). The widths of the tube along different projections reflect the measured amplitude interplay $P_{12} > 0$, $P_{22} < 0$, with the fast block contributing most of the curvature. Because the angles advance at an irrational ratio, the trajectory never closes. The 2D projections are not lines but "densely filled bands", such as the (u-v) region defined by u between 0.59-0.65 and v between 0.91-0.98. The visual contrast with the rational case underscores the role of the rotation number in shaping the flow.

Remark 2. A central finding of this work is the failure of Lyapunov stability at the steady-state equilibrium. This failure is a direct consequence of a significant degeneracy in the cubic normal-form coefficients. The standard non-degeneracy condition for a generic double Hopf bifurcation requires that all amplitude coefficients are non-zero, formally stated as

$$(\operatorname{Re} G_{2100}) (\operatorname{Re} G_{1011}) (\operatorname{Re} G_{1110}) (\operatorname{Re} G_{0021}) \neq 0.$$

Our analysis reveals that the dynamical system violates this standard condition. Specifically, our numerical evaluation robustly demonstrates that the first Lyapunov coefficients (the self-coupling terms) are numerically zero:

$$P_{11} = \text{Re}(G_{2100}) \approx 0, \qquad P_{21} = \text{Re}(G_{1110}) \approx 0.$$

This degeneracy $(P_{11} \approx 0, P_{21} \approx 0)$ is fundamental. It implies that the oscillatory modes, corresponding to the amplitudes r_1 (Goodwin cycle) and r_2 (underemployment cycle), lack intrinsic self-damping or self-saturation mechanisms at the cubic order. Consequently, the local dynamics are entirely dictated by the nonlinear cross-coupling structure in the amplitude equations:

$$\begin{split} r_1' &= r_1 \left(\frac{1}{2} P_{11} r_1^2 + P_{12} r_2^2 \right) \approx r_1 \left(P_{12} r_2^2 \right), \\ r_2' &= r_2 \left(P_{21} r_1^2 + \frac{1}{2} P_{22} r_2^2 \right) \approx r_2 \left(\frac{1}{2} P_{22} r_2^2 \right). \end{split}$$

Our computations yield a consistent sign pattern for the non-zero coupling coefficients: $P_{12} > 0$ and $P_{22} < 0$. This structure defines the flow:

• The r_2 mode is self-limiting ($P_{22} < 0$), saturating its own amplitude.

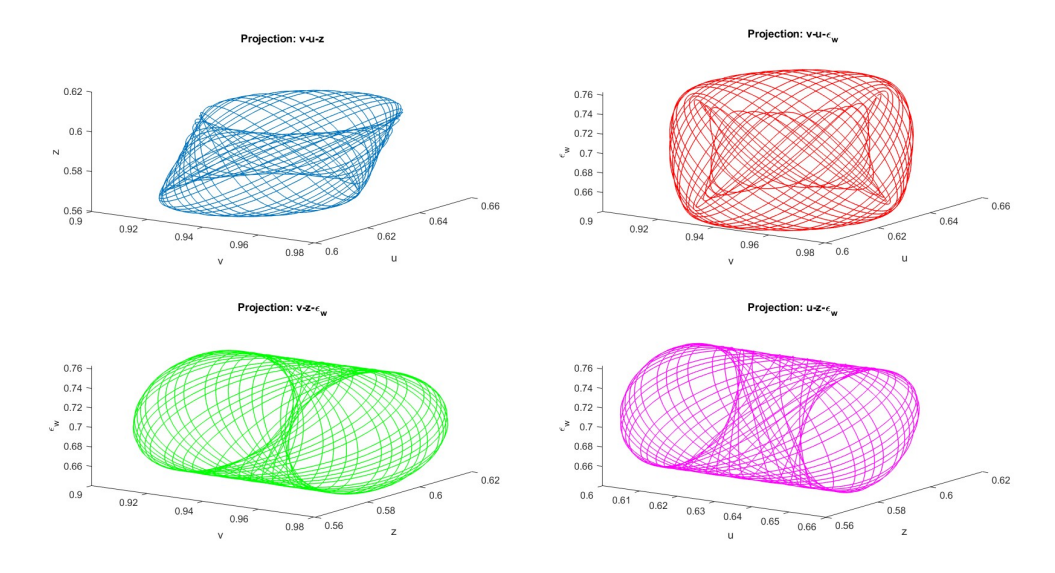


Figure 14: Comprehensive 3D projections of the system for the non resonance case but with irrational ratio ($\chi \approx 0.16453$).

• The r_1 mode, lacking self-damping, is driven by a positive (destabilizing) cross-feeding term from the r_2 mode ($P_{12} > 0$).

This interaction generates an expansive flow (outward drift) in the amplitude phase space, rendering the equilibrium a repulsor (or a saddle-type instability on the center manifold). The local instability, guaranteed by this cubic degeneracy, is precisely the mechanism that necessitates the evolution of trajectories away from the origin and onto the non-trivial, bounded attractors (the synchronized limit cycles and quasi-periodic tori) documented in Section 6. This diagnostic is robust at the third order.

7. Conclusion

This paper has developed and analyzed an extension of the Goodwin model of endogenous distributive cycles that incorporates the joint dynamics of wage inequality and underemployment, conceived as a regime of low productivity, low wages, and weak bargaining power. The economy comprises two classes of workers, treated as perfect substitutes in production but differentiated by productivity, wage levels, and bargaining strength. Type 1 workers occupy high-productivity positions, whereas type 2 workers are employed in low-productivity ones. The growth rate of real wages for each labor type depends positively on its share in total employment. However, the lower bargaining power of type 2 labor entails systematically smaller wage adjustments relative to type 1 labor, generating persistent wage inequality.

The distribution of the labor force between these two groups is summarized by an endogenous underemployment rate, whose evolution is represented by a simplified power-balance mechanism between capitalist firms—seeking to exploit the lower cost of type 2 labor—and workers collectively striving to improve labor conditions. Integrating these components yields a four-dimensional dynamical system that extends Goodwin's original two-dimensional formulation. Alongside the wage share and the employment rate, the relative wage of type 2 workers and the underemployment rate emerge as additional state variables. The existence and uniqueness of solutions for this system have been proved through fixed-point theory, and the steady-state equilibrium is shown to be non-hyperbolic, implying the absence of intrinsic self-stabilizing forces that make the economy converge to an equilibrium point.

A theoretical contribution of this paper is the identification of a double Hopf bifurcation in the model, providing a formal explanation for the coexistence and interaction of two endogenous oscillatory modes. The first corresponds to the Goodwin cycle, driven by the feedback between the wage share and the employment rate. The second, denoted as the underemployment cycle, arises from the interaction between the underemployment rate and the relative wage

of type 2 workers. The analytical classification of resonant and nonresonant regimes illustrates how these cycles interact. In the nonresonant case, the Goodwin and underemployment cycles operate at distinct frequencies, producing quasi-periodic fluctuations. This regime may represent an economy in which capital accumulation and labor-market segmentation evolve asynchronously, generating bounded but complex oscillations. Under resonance, by contrast, the two cycles become synchronized, producing amplified and coherent fluctuations in income distribution, employment, wage inequality, and underemployment. Mathematically, these correspond to the 1:1, 1:2, and 1:3 resonant Hopf-Hopf bifurcations derived analytically and confirmed through numerical simulation.

The numerical simulations performed with Matlab corroborate the theoretical findings. The frequency-ratio curve ω_1/ω_2 exhibits the predicted resonant points, while the bifurcation diagram of the local maxima of the employment rate reveals alternating regions of regular and complex dynamics. Narrow periodic windows occur near resonant ratios, indicating synchronized cycles, whereas nonresonant intervals produce dense quasi-periodic trajectories. As the adjustment speed of underemployment (χ) increases, the simulated patterns reproduce the resonance structures predicted by the cubic normal form. The normal-form analysis on the center manifold further clarifies the local properties of the system. The signs of the cubic coefficients (P_{ij}) determine whether oscillations remain bounded or evolve toward irregular regimes, while the non-vanishing resonant coefficients (G_1, G_2) account for the emergence of loworder resonances and phase closure in planar projections. Altogether, these results capture several dynamic regimes, ranging from regular Goodwin-type cycles to complex multi-frequency oscillations.

The paper also contributes to the literature on endogenous macroe-conomic fluctuations by proposing an alternative framework that links distributive cycles and wage inequality within a heterodox analytical perspective. The interaction between accumulation and labor-market segmentation, embodied by the dual cyclical structure of the model, provides a formal mechanism through which wage inequality and underemployment arise endogenously as components of the capitalist growth process. The identification of resonant double Hopf bifurcations offers a basis for understanding how structural parameters, such as saving behavior, labor-market configuration, and bargaining asymmetries, can shift the economy from regular to irregular cyclical regimes. Taken together, the analytical and numerical results indicate that capitalist economies, as represented by this model, may sustain multiple layers of endogenous cyclical motion

Finally, this framework opens several avenues for future research. A potential extension would be to examine the sensitivity of endogenous cycles to additional stabilizing mechanisms, such as collective bargaining institutions, fiscal and monetary policy, or external demand constraints. Empirical calibration using data on wage inequality and employment conditions could further evaluate the explanatory and predictive capacity of the model. Moreover, extending the analysis to include financial variables or endogenous technical change may provide additional intuitions about the functioning of income distribution, cyclical employment fluctuations, and the long-run evolution of capitalist macrodynamics.

Declaration of generative AI and AI-assisted technologies in the writing process

During the preparation of this work the authors used ChatGPT to enhance the writing quality. After using this tool/service, the authors reviewed and edited the content as needed and take full responsibility for the content of the publication.

This research did not receive any specific grant from funding agencies in the public, commercial, or not-for-profit sectors.

CRediT authorship contribution statement

John Cajas-Guijarro: Writing – review & editing, Writing – original draft, Visualization, Software, Formal analysis, Conceptu-

Daniel Cajas-Guijarro: Writing – review & editing, Visualization, Software, Formal analysis.

Declaration of competing interest

The authors declare that they have no known competing financial interests or personal relationships that could have appeared to influence the work reported in this paper.

Data availability

No data was used for the research described in the article.

References

- D. Autor. Work of the past, work of the future. AEA Papers and Proceedings, 109:1–32, 2019
- D. Acemoglu and P. Restrepo. Task *Econometrica*, 90(5):1973–2016, 2022. Tasks, automation, and the rise in u.s. wage inequality.
- Leonardi M. Koeniger, W. and L. Nunziata. Labor market institutions and wage inequality. Industrial and Labor Relations Review, 60(3):340–356, 2007.
- Lemiex T. Card, D. and C. Riddell. Unions and wage inequality: The roles of gender, skill and [4] plic sector employment. Canadian Journal of Economics, 53(1):140-173, 2020. [5]
- D. Card and T. Lemieux. Can falling supply explain the rising return to college for you a cohort-based analysis. *The Quarterly Journal of Economics*, 116(2):705–746, 2001.

 Marco Stamegna. Wage inequality and induced innovation in a classical-marxian growth model.
- [6] nal of Evolutionary Economics, 34(1):127-168, January 2024.
- R. Blecker and M. Setterfield. *Heterodox Macroeconomics*. Edwad Elgar, Cheltenham, 2019.
- T. Palley. Wage- vs. profit-led growth: the role of the distribution of wages in determining regin character. *Cambridge Journal of Economics*, 41(1):49–61, 2017. [8]
- T. Palley. Capitalists, workers, and managers: Wage inequality and effective demand. Structural Change and Economic Dynamics, 30:120–131, 2014. [9]
- Charles S. Dutt, A.K. and D. Lang. Employment flexibility, dual labour markets, grodistribution. *Metroeconomica*, 66(4):771–807, 2015. [10] [11]
- A.K. Dutt and R. Veneziani. Education and 'human capitalists' in a classical-marxian model of growth and distribution. *Cambridge Journal of Economics*, 43(2):481–506, 2019. [12] C. Kennedy. Induced bias in innovation and the theory of distribution. The Economic Journ
- (295):541–547, 1964. elson. A theory of induced innovation along kennedy-weisäcker lines. The Review of [13]
- nics and Statistics, 47(4):343–356, 1965.
- R. M. Goodwin. A Growth Cycle, pages 54–58. Cambridge University Press, Cambridge, 1967.
- A. Shah and M. Desai. Growth cycles with induced technical change. The Economic Journ [15] 91:1006-1010, 1981.
- F. van der Ploeg. Growth cycles, induced technical change, and perpetual conflict over the [16] distribution of income. *Journal of Macroeconomics*, 9:1–12, 1987.

 John Cajas Guijarro. An extended goodwin model with endogenous technical change and labor
- [17] ly. Structural Change and Economic Dynamics, 70:699-710, 2024. [18]
- J. Glombowski and M. Krüger. A short-period growth cycle model. Recherches Économiques de Louvain/Louvain Economic Review, 54:423–438, 1988. P. Skott. Effective demand, class struggle and cyclical growth. International Economic Review, [19]
- Tavani D. von Arnim R. Rada, C. and L. Zamparelli. Classical and keynesian models of inequality [20]
- and stagnation. *Journal of Economic Behavior Organization*, 211:442–461, 2023.

 M. Desai. Growth cycles and inflation in a model of the class struggle. *Journal of Economic Behavior Organization*, 211:442–461, 2023. [21] ory, 6(6):527-545, 1973.
- [22] Y. Sato. Marx-goodwin growth cycles in a two-sector economy. Journal of Economics, 45(1):21-
- J. Caias Guijarro. A classical marxian two-sector endogenous cycle model. Metroeconomica. [23] S. Keen. Finance and economic breakdown: Modeling minsky's "financial instability hypothe [24]
- Journal of Post Keynesian Economics, 17(4):607-635, 1995. S. Sordi and A. Vercelli. Unemployment, income distribution and debt-financed investment in a [25]
- [26]
- P. Manfredi and L. Fanti. Demography in macroeconomic models: When labour supply matters for economic cycles. *Metroeconomica*, 57(4):536–563, 2006. P. Flaschel and A Greiner. Employment cycles and min mum wages, a macro view. Structural

- [28] M. Dávila-Fernández and S. Sordi. Distributive cycles and endogenous technical change in wth model. *Economic Modelling*, 77:216–233, 2019.
- M. Sportelli and L. De Cesare. A goodwin type cyclical grow Strucutral Change and Economic Dynamics, 61:95–102, 2022.
- [30] G Bella. Emergence of chaotic dynamics in the goodwin model with disequilibrium in the goods
- Mendieta-Muñoz I. Rada C. Tavani D. Barrales-Ruiz, J. and R. von Arnim. The distributive cycle: Evidence and current debates. *Journal of Economic Surveys*, 36(2):468–503, 2022.
- P. Flaschel and A. Greiner. Dual labor markets and the impact of minimum wages on atypical nployment. Metroeconomica, 62(3):512-531, 2011.
- R. Solow. A contribution to the theory of economic growth. *The Quarterly Journ* 70(1):65–94, 1956.
- Greiner A.-Logeay C. Flaschel, P. and C. Proaño. Employment cycles, low income work and the dynamic impact of wage regulations, a macro perspective. Journal of Evolutionary Econol 2-235_250 2012
- Asada Y. Sasaki, H. and R. Sonoda. Effects of minimum wage share and wage gap reduction on [35] cyclical fluctuation: A goodwin approach. Technical Report 121695, MPRA, 2015. preprin Marsuyama J. Sasaki, H. and K. Sako. The macroeconomic effects of the wage gap betw
- [36] regular and non-regular employment and of minimum wages. Structural Change of Dynamics, 26:61–72, 2013.
- H. Sasaki. Profit sharing and its effect on income distribution and output: a kaleckian approach Cambridge Journal of Economics, 40(2):469–489, 2016.
- M. Grasselli and A. Maheshwari. Testing a goodwin model with general capital accu te. Metroeconomica, 69, 2018.
- M. Kalecki. Political aspects of full employment. The Political Quarterly, 14, 1943.
- [40] P. YU. Closed-form conditions of bifurcation points for general differential equa al Journal of Bifurcation and Chaos, 15(04):1467–1483, 2005.
- P. C. PARKS. A new proof of hermite's stability criterion and a generalization of orlando's [41] ional Journal of Control, 26(2):197–206, 1977.
- Yu. A. Kuznetsov. Numerical normalization techniques for all codim 2 bifurcations of equilibria [42] e's. SIAM Journal on Numerical Analysis, 36(4):1104–1124, 1999
- [43] Yu. A. Kuznetsov. Elements of Applied Bifurcation Theory. Applied Mathematical Sciences ger, Germany, 4th edition, 2023.
- Henk Broer, Heinz Hanßmann, and Florian Wagener. Normal resonances in a double hoof [44]
- bifurcation. *Indagationes Mathematicae*, 32(1):33–54, 2021.

 S. Caprino, C. Maffei, and P. Negrini. Hopf bifurcation at 1:1 resonance. *Nonlinear Analysis*: [45] ions, 8(9):1011-1032, 1984.
- Theory, memory approximately proceedings of the Royal Society of London. Series A, Mathematical and Physical Sciences, 415:61–90, 1988 [46]
- [47] V. G. LeBlanc and W. F. Langford. Classification and unfoldings of 1:2 resonant hopf bifurcation
- Achive for Rational Mechanics and Analysis, 136:305–357, 1996.

 A. Luongo, A. Paolone, and A. Di Egidio. Multiple timescales analysis for 1:2 and 1:3 resonant [48] f bifurcations. Nonlinear Dynamics, 34:269-291, 2003.
- nopi Diurcations, Nominear Dynamics, Server Mateont: A matlab package for numerical bifurcation analysis of odes. ACM Trans. Math. Softw., 29(2):141–164, June 2003. [49]
- A. Dhooge, W. Govaerts, Yu. A. Kuznetsov, H. G.E. Meijer, and B. Sautois. New features of the [50] mical systems. Mathematical and Computer Modelling of Dynamical Systems, 14(2):147-175, 2008.

Centro de Investigación en Ingeniería Matemática (CI²MA)

PRE-PUBLICACIONES 2025

- 2025-14 Gabriel N. Gatica, Zeinab Gharibi, Ricardo Oyarzúa: Banach spaces-based fully mixed finite element methods for the n-dimensional Boussinesq problem with temperature-dependent parameters
- 2025-15 SERGIO CAUCAO, RICARDO OYARZÚA, SEGUNDO VILLA-FUENTES: A priori and a posteriori error analyses of a fully-mixed finite element method for the coupled Navier Stokes / Darcy problem
- 2025-16 Juan Barajas-Calonge, Raimund Bürger, Pep Mulet, Luis M. Villada: A second-order invariant-region-preserving scheme for a transport-flow model of polydisperse sedimentation
- 2025-17 RAIMUND BÜRGER, STEFAN DIEHL, MARÍA CARMEN MARTÍ, YOLANDA VÁSQUEZ: A numerical scheme for a model of a flotation column including the transport of liquid components
- 2025-18 RAIMUND BÜRGER, ENRIQUE D. FERNÁNDEZ NIETO, JOSÉ GARRES-DÍAZ, JORGE MOYA: Well-balanced physics-based finite volume schemes for Saint-Venant-Exner-type models of sediment transport
- 2025-19 HAROLD D. CONTRERAS, PAOLA GOATIN, LUIS M. VILLADA: Well-posedness of a nonlocal upstream-downstream traffic model
- 2025-20 Thierry Coulbois, Anahi Gajardo, Pierre Guillon, Victor H. Lutfalla: Aperiodic monotiles: from geometry to groups
- 2025-21 ESTEBAN HENRIQUEZ, TONATIUH ŠANCHEZ-VIZUET, MANUEL SOLANO: An unfitted HDG discretization for a model problem in shape optimization
- 2025-22 FERNANDO ARTAZA-COVARRUBIAS, TONATIUH SANCHEZ-VIZUET, MANUEL SOLANO: A coupled HDG discretization for the interaction between acoustic and elastic waves
- 2025-23 ÉIDER ALDANA, RICARDO OYARZÚA, JESÚS VELLOJÍN: Numerical analysis of a three-field formulation for a reverse osmosis model
- 2025-24 Julio Aracena, Florian Bridoux, Maximilien Gadouleau, Pierre Guillon, Kevin Perrot, Adrien Richard, Guillaume Theyssier: On the Dynamics of Bounded-Degree Automata Networks
- 2025-25 Daniel Cajas Guijarro, John Cajas Guijarro: Resonant and non-resonant double Hopf bifurcation in a 4D Goodwin model with wage inequality

Para obtener copias de las Pre-Publicaciones, escribir o llamar a: DIRECTOR, CENTRO DE INVESTIGACIÓN EN INGENIERÍA MATEMÁTICA, UNIVERSIDAD DE CONCEPCIÓN, CASILLA 160-C, CONCEPCIÓN, CHILE, TEL.: 41-2661324, o bien, visitar la página web del centro: http://www.ci2ma.udec.cl









CENTRO DE INVESTIGACIÓN EN INGENIERÍA MATEMÁTICA (CI²MA) Universidad de Concepción

Casilla 160-C, Concepción, Chile Tel.: 56-41-2661324/2661554/2661316 http://www.ci2ma.udec.cl





